A partial skeleton of "*Mammut*" *borsoni* (Proboscidea, Mammalia) from the Pliocene of Kaltensundheim (Germany)

Wighart v. Koenigswald, Jakub Březina, Ralf Werneburg, and Ursula B. Göhlich

ABSTRACT

A detailed description of a partial skeleton of "*Mammut*" *borsoni* from the late Pliocene (Early Villafranchian, MN 16/17) of Kaltensundheim in Thuringia (Germany) is provided, and concentrates on osteological comparisons with specimens of the European Mammutidae (*Zygolophodon turicensis* and "*M*". *borsoni*) and the North American *Mammut americanum*. Osteological similarities between "*M*". *borsoni* and *M. americanum* have to be regarded as parallelisms. The Kaltensundheim specimen is one of the youngest appearances of mammutids in Europe. The skeleton may represent a female, because it is distinctly smaller than male individuals from Milia in Greece of a similar ontogenetic age.

We use the genus name "*Mammut*" in quotation marks, because the genus *Mammut* evolved in North America and no reinvasion into Eurasia can be proven. Therefore, the genus name *Mammut* should not be used prematurely for Eurasian finds.

Wighart v. Koenigswald. Universität Bonn, Institut für Geowissenschaften (Paläontologie), Nussallee 8, D-53115 Bonn, Germany. koenigswald@uni-bonn.de
Jakub Březina. Department of Geological Sciences, Faculty of Sciences, Masaryk University, Kotlářská 267/2, 611 37, Brno, Czech Republic and Department of Geology and Paleontology, Moravian Museum, Zelný trh 6, 659 37 Brno, Czech Republic. jbrezina@mzm.cz
Ralf Werneburg. Naturhistorisches Museum, Schloss Bertholdsburg, Burgstraße 6, D-98553 Schleusingen, Germany. werneburg@museum-schleusingen.de
Ursula B. Göhlich. Naturhistorisches Museum Wien, Geologisch-paläontologische Abt., Burgring 7, A-1010 Wien, Austria. ursula.goehlich@nhm-wien.ac.at

Key words: Mammutidae; "*Mammut*" *borsoni*; osteology; sexual dimorphism; Pliocene; Eurasia

INTRODUCTION

Mammutids are one of the proboscidean families that roamed Eurasia during the Neogene, from the early Miocene (Mammal Neogene unit MN3b) at about 18-17 Ma (Tassy, 1990; Göhlich, 2010; van der Made, 2010) until the earliest Pleistocene (MN17) at about 2.5-2.0 Ma (Virág and Gasparik, 2012). The Mammutidae originated in Africa during the late Oligocene (Rasmussen and Gutierrez, 2009; Sanders et al., 2010; Tassy, 2018) invaded Eurasia via the Arabian Peninsula and the *"Gomphotherium* land bridge" during the early Miocene (Tassy, 1990; Rögl, 1999; Harzhauser et al. 2007) and subsequently immigrated via Asia (Duangkrayom et al., 2017) into North America during the late early Miocene via the Bering land bridge (Prothero et al., 2008; Lofgren and Anand 2011). In North America the mammutid lineage terminated in the iconic American mastodon *Mammut americanum* (Kerr, 1792) that experienced a heyday during the late Pleistocene and is eponymous for the family Mammutidae (Zazula et al., 2014; Widga et al., 2017).

Among proboscideans, Mammutidae are characterized by their zygodont molar pattern (Tobien, 1975, 1996). The cheek teeth of Mammutids stay morphologically very conservative throughout their evolution, and thus the differentiation of species is difficult. Furthermore, mammutid fossils (especially complete skeletons) are in general very rare in Eurasia, much rarer than those of gomphotheres or deinotheres. The cranial morphology of Eurasian mammutids is almost unknown and relatively complete dentitions, mandibles, or maxillas are barely found. Most findings are isolated molars. These factors impede the identification and definition of different mammutid taxa and the deduction on their phylogeny. Therefore, the detailed description of the partial skeleton of the *"Mammut" borsoni* individual from the late Pliocene of Kaltensundheim (Germany) and its comparisons with some specimens of Mammutidae (*Zygolophodon turicensis, "M". borsoni, M. americanum)* presented herein can serve to solve taxonomic or phylogenetic questions of this poorly understood group of proboscideans.

The earliest mammutid species in Europe is *Zygolophodon turicensis* (Schinz, 1824), which appeared during the early Miocene in MN3b at about 18-17 Ma (Tassy, 1990; Göhlich, 2010) and may have persisted until MN10, e.g., in Soblay (France) (Tassy, 1985; Göhlich, 1999). In Spain, however, *Zygolophodon* is supposed to be extinct by MN8 (Mazo and van der Made, 2012). The ter-

minal taxon of Mammutids in Eurasia is the so-called Borson's mastodon, most widely known under the binomen *"Mammut" borsoni* (Hays, 1834), which persisted until the earliest Pleistocene (MN17).

Several other mammutid species and genera preceding *"M". borsoni* were described from the Neogene of Europe (e.g., Nikolov and Kovačev, 1966; Kubiak, 1972; Markov 2004, 2008) and Asia (e.g., Mothé et al., 2016; Wang et al., 2020; Zhang and Wang, 2021). For several of these species the taxonomic identity and validity is, however, under debate, because of incomplete materials that provide only a limited number of characters. Unravelling these problems is not the scope of this paper. Nevertheless, we provide a survey of the European finds including measurements and stratigraphic positions in order to provide an outline for detailed discussions. Also, the affiliation of the Borson's mastodon to the genus has been under debate since long. It was originally described by Hays (1834) as *Mastodon borsoni,* but was subsequently referred either to the basal genus *Zygolophodon* Vacek, 1877 (e.g., Schlesinger, 1917, 1922; Schaarschmidt, 1958; Bergounioux and Crouzel, 1961; Mein, 1990; Saunders, 1996; Rakovec, 1997; Tassy, 1985; Vislobokova and Sotnikova, 2001; Vislobokova, 2005) or to *Mammut* Blumenbach, 1799 (e.g., Fejfar, 1964; Kubiak, 1972; Tobien, 1975, 1977, 1996; Kahlke, 1995; Tsoukala, 2000; Tsoukala et al., 2010; Karl et al., 2013; Tsoukala and Mol, 2016; Larramendi, 2016). The type species of the genus *Mammut* Blumenbach, 1799, however, is *M. americanum* (Kerr, 1792), the American mastodon. It is based on isolated molars found in 1739 near the Ohio River in Northern Kentucky (Tassy, 2002).

To date, the reconstruction of the phylogeny of mammutids and possible migration scenarios between Eurasian and North American taxa is encumbered with uncertainties, because of various reasons: the fossil record is limited; a series of dubious taxa was described: some of them are questioned in their taxonomic validity; finally, any evidence is missing that mammutids migrated between Eurasia and North America more than once, although required for some phylogenetical reconstructions.

It is generally accepted that *"M". borsoni* in Eurasia and *Mammut americanum* from North America represent terminal species of two independent and geographically separated phylogenetic lineages (e.g., Saunders 1996; Tassy, 1996a; Shoshani and Tassy, 1996; Markov 2004) and

hypothesis of the second late Miocene-Pliocene migration of *Mammut* to North America favored by e.g., Schlesinger (1922) or Tobien (1977, 1996) is unsufficiently supported. It is unlikely that the two lineages separated since the early Miocene represent the same genus. As a consequence, the genus name *Mammut* is not available for the Eurasian taxon, because otherwise it would implicate a polyphyletic origin for the genus *Mammut*. Recently, some other mammutid genera were described or mentioned from Asian deposits. However, the validity of the newly established mammutid genus *Sinomammut* Mothé, Avilla, Zhao, Xie, and Sun, 2016, or the occurrence of the actually North American genus *"Miomastodon"* (Wang et al., 2020) or of the African genus *Eozygodon* (Zhang and Wang, 2021) in Asia requires further extensive analyses, which are out of the scope of this publication. For the time being, it has to remain open, if *"M". borsoni* might belong to one of these genera or represents a so far undescribed genus. Therefore, we follow Markov (2004, 2008) in his provisional taxonomical solution *"Mammut" borsoni,* writing the generic name in quotation marks.

The Sinkhole of Kaltensundheim, Locality and Age of the Filling

The partial skeleton described here was discovered in a former sinkhole near Kaltensundheim on the eastern slope of the Rhön Mountains in southern Thuringia, Germany (Figure 1). The sinkhole is located on the northwestern margin of the village Kaltensundheim on the southern side of Lotte River. Its position is documented by maps and photos. The coordinates are 50.610748 N, 10.153696 E (or in traditional geographic coordinates 50°37' N, 10°09' E). The sinkhole is formed within Middle Triassic limestone (unterer Muschelkalk, Wellenkalk), which overlies the Lower Triassic Buntsandstein. Its uppermost part, the Röt Formation, contains gypsum and salt. Intensive karstic underground dissolution of these minerals caused a collapse of Muschelkalk limestones and formation of a number of sinkholes (Böhme, 1963, 1992). The geologist Klaus Duphorn (later Univ. Kiel) reconstructed the oval shape of the Kaltensundheim sinkhole with a 1 m long iron probe (Figure 1D) (Böhme, 1968, 1992). The maximal diameter is of about 100 m in a north-south direction. The depth is not known, but trenches of 10 m depth did not reach the basement.

A thin overburden of less than 0.5 m contains some fluviatile gravels. The fossiliferous sinkhole fill consists of fine grained and layered sediments.

The upper section of up to 1.8 m is a yellow-brownish to red-brownish loam with Fe-Mn concretions, whereas the lower part is a blackish clay. The difference in color between the two sections is due to sub-surface bleaching. In the section exposed during the excavation, layers were observed to be inclined at about 35° towards the center of the sinkhole following the natural slope (Böhme, 1992). The skeletons were imbedded in the brownish section parallel to the sloping beds. In some parts, the sinkhole stratigraphy was complicated by intensive sediment slumping from the edges. Coloration of the soil indicates also the presence of a second, unexcavated sinkhole, about 500 m in a northwesterly direction of the first sinkhole (Böhme, 1992).

In December 1957, large fossil bones were discovered during construction activities for the nearby farm leading to excavations the following year. In 1958, the former Museum in Meiningen (Thuringia) excavated the mammutid skeleton (studied here) under the supervision of Friedemann Schaarschmidt (later Senckenberg Museum, Frankfurt a. M.) (Figure 2). A second campaign took part in 1962-1966 lead by Gottfried Böhme (later Museum für Naturkunde, Berlin) and produced the skeleton of a small deer *Avernoceros ardei* (Böhme, 1963; Pfeiffer-Deml, 2020). In 1976 to 1978, a third campaign in the same sinkhole was executed by the Institut für Quartärpaläontologie in Weimar under the direction of Hans-Dietrich Kahlke. It yielded a second partial mammutid skeleton containing straight upper tusks. This second individual is stored at the SFQW in Weimar and was not accessible for this study. The two mammutid individuals have not yet been published in detail; the literature related to Kaltensundheim is limited to excavation maps and field reports (Schaarschmidt, 1958; Böhme, 1963, 1968, 2002, 2007; H.-D. Kahlke, 1981; R.-D. Kahlke, 1995, 1998). A description of the first skeleton of *"M". borsoni* excavated in 1958 is presented here.

The Villafranchian age of the filling in the Kaltensundheim sinkhole is indicated by three mammalian species *Hypolagus brachygnathus, Arveroceros ardei,* and *"Mammut" borsoni* (Böhme, 2002; Pfeiffer-Deml, 2020) and by a Late Pliocene flora with 70 species. This flora was correlated to Ceyssac in the French Massif Central. The age of this "Ceyssac-Kaltensundheim flora" is assumed as 2.8 Ma to 2.56 Ma (Gümbel and Mai, 2004; Mai, 2007; Böhme, 2007). This time slice includes the Pliocene-Pleistocene boundary at about 2.6 Ma and equals MN16 or MN17 in the European mam-
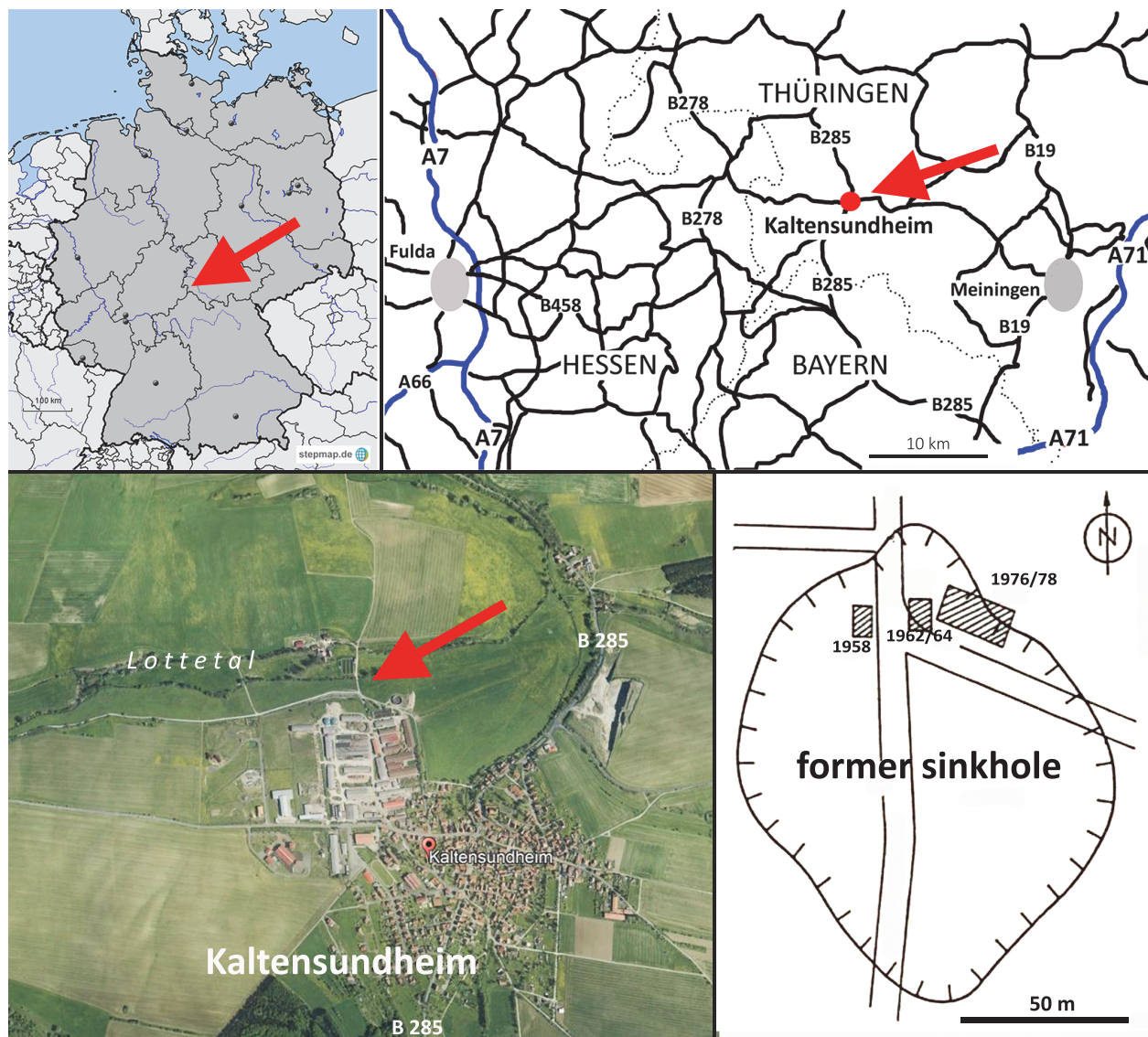
FIGURE 1. A-C: Maps showing the geographic situation of the Kaltensundheim sinkhole north of the farm in the village Kaltensundheim (Thuringia) in Germany. **D:** Plan of the excavation pits in the former sinkhole (Böhme, 1992). (Figure 1C modified from GoogleEarth).

mal chronology (Hilgen et al., 2012) (Figure 3). Thus, the *"M". borsoni* is slightly younger than the finds from Vialette (F) and Hajnáčka (SK) assigned to MN16 (Fejfar, 1964; Lacombat et al., 2008). The latest occurrences of *"M". borsoni* in Central Europe are documented from Strekov and Nová Vieska (SK) (Holec, 1985, 1996; Vlačiky et al., 2008) and some Hungarian localities near Budapest (Gasparik, 2001; Virág and Gasparik, 2012), all dated as MN16-MN17.

The sinkhole fill was deposited in a small lake, as indicated by remains of fishes (*Esox lucius*, cf. *Tinca, Rutilus* sp.) and amphibians *(Bufo bufo,*

Bufo sp., and *Rana temporaria*). The sidewalls of the sinkhole formed by the bedrock are very steep. Thus, the sinkhole, most probably, formed a natural trap for small and large mammals (*Hypolagus* sp., *Avernoceros ardei*, and *"M". borsoni*) (Böhme, 1963, 1992, 2002). This interpretation is confirmed by the relative completeness of the skeletons.

Beside this material from Kaltensundheim, other localities in Thuringia and the Rhön area only produced a few isolated molars of *"M". borsoni* (Kahlke, 1995; Braniek, 1995). Therefore, the skeletons from the Kaltensundheim sinkhole are exceptional.
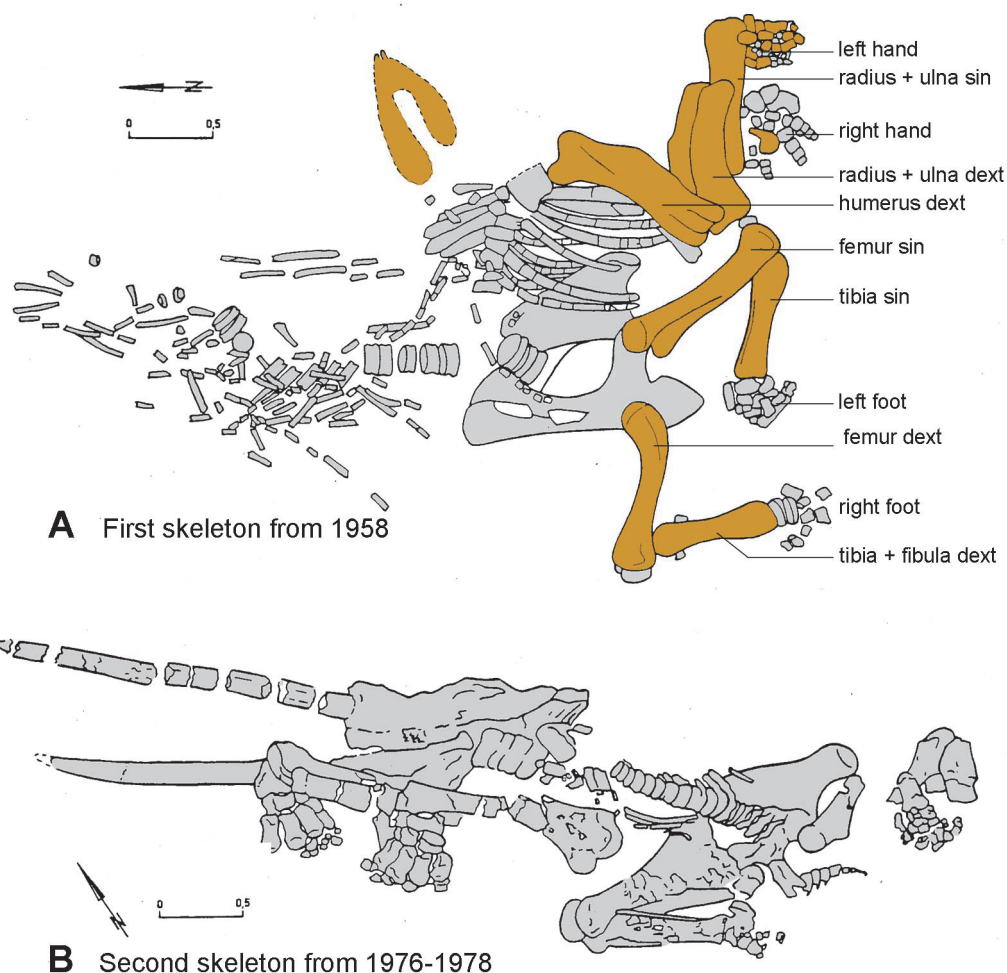
FIGURE 2. Excavation sketches of two *"Mammut" borsoni* individuals from the Kaltensundheim sinkhole. **A:** The specimen excavated in 1958 is discussed in this paper. Yellow-shaded bones are housed in the NHMS (MTe 810) and are described below. The whereabouts of the other bones is unknown. **B:** The second individual excavated in 1976-1978 is housed at the SFQW (modified from Kahlke, 1985) and was not available for this study.

MATERIALS AND METHODS

The partial skeleton from the Kaltensundheim sinkhole excavated in 1958 is stored in NHMS in Schleusingen, under the inventory numbers NHMS-MTe 810/1 to 37. After its excavation, it was exhibited in the local Museum in Meiningen (Figure 4A), subsequently moved partially to Weimar. In 1988, it was transferred to the Naturhistorisches Museum Schloss Bertholdsburg in Schleusingen (Thuringia). The available material is noticeably less complete than in published excavation plans (Figure 2). Therefore, it is possible that some other skeletal elements of this individual remained unrecognized in other collections.

In the following, for convenience, only the last number of the inventory acronym (NHMS-MTe 810) referring to the individual bones is shown in brackets:

Mandible with Dentition (NHMS-MTe 810/1)

Forelimb. Small scapula fragment (17), humerus dext (6), humerus sin (2), ulna dext (3a), ulna sin (7a), radius dext (3b), and sin (7b).

Manus. Scaphoideum sin (21), lunatum sin (20), cuneiforme dext (24), pisiforme sin (23), trapezium sin (33), trapezoideum sin (32), capitatum sin (22), hamatum sin (25), metacarpale primum sin (34), metacarpale secundum sin (35), metacarpale tertium sin (29), metacarpale quartum sin (28), prox. phalanx 2 sin (36), prox. phalanx 3 sin (30), prox. phalanx 4 sin (26), med. phalanx 2 sin (37), med. phalanx 3 sin (31), med. phalanx 4 sin (27).

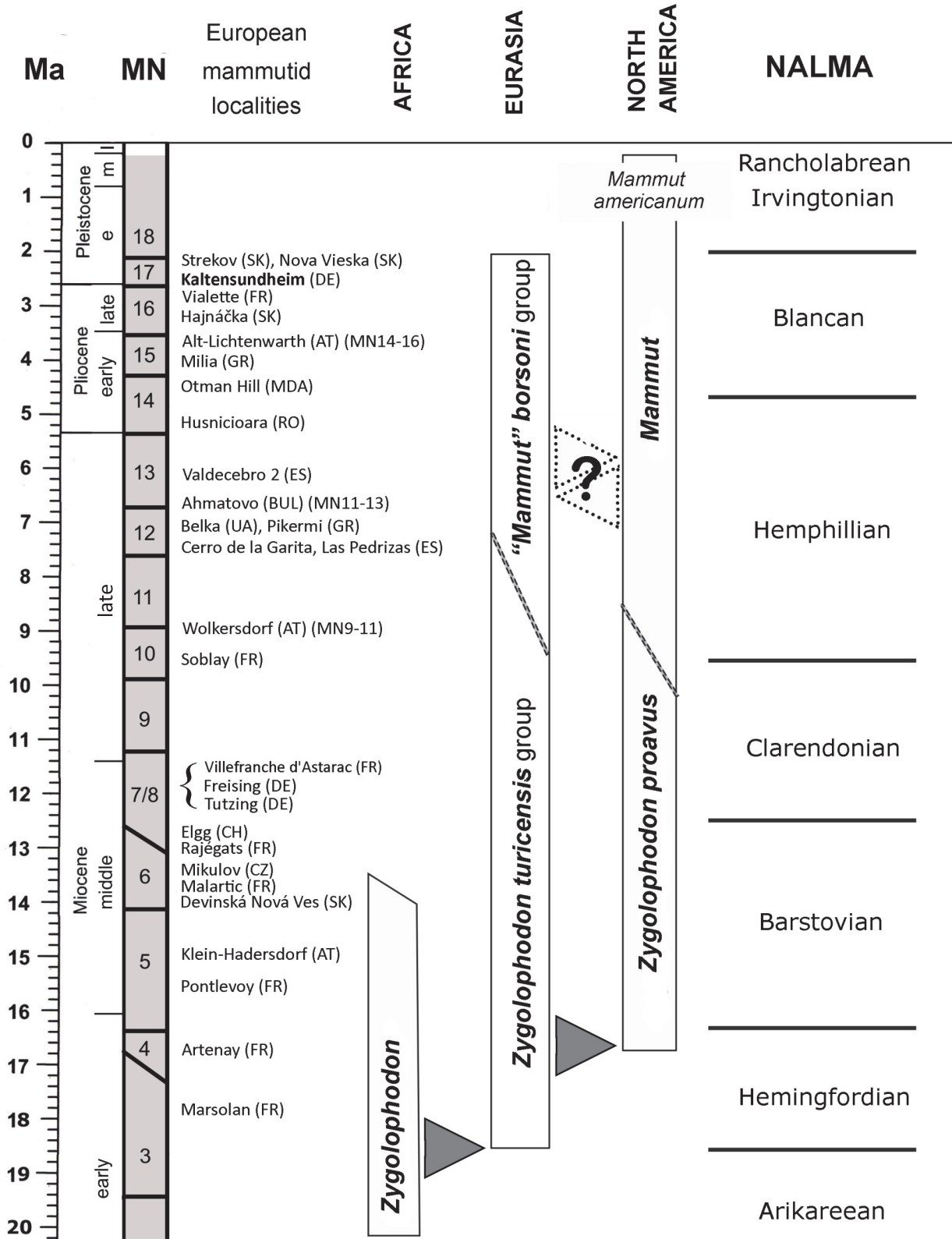**FIGURE 3.** Stratigraphic position of important European localities with *Zygolophodon* and *"Mammut",* and the expansion of *Zygolophodon* from Africa to Eurasia and to North America. A second immigration of Mammutidae to North America cannot be proven. NALMA - North American Land Mammal Ages; MN - European Neogene mammals Zones and stratigraphic scale in million years according to (Hilgen et al., 2012).

FIGURE 4. *"Mammut" borsoni* from Kaltensundheim. **A:** Historical photo (prior to 1988) of the mounted left arm and the mandible of the first *"Mammut" borsoni* at a temporary exposition in Meiningen with Dr. Böhme. In the unrestored mandible the two original mandibular tusks are obvious. **B:** The actual state of the mandible with reconstructed tusks in the exhibition of the NHMS in 2017.

Hindlimb. Femur dext (8), femur sin (4), tibia dext (9), tibia sin (5a), fibula sin (5b).

We provide 3D images of the mandible and selected longbones on MorphoSource.

Preservation and Preparation

According to the excavation plan (Figure 2) the bones were found in close articulation without any traces of transport. Therefore, the bones clearly belong to a single individual. All long bones were fractured by compacting sediments but were restored to a convincing general shape. The stability of some bones was improved by inserting metal sticks inside the bones during preparation (Figure 5B). The bones were consolidated with Geiseltallack (polymere cellulose nitrate) and missing portions have been sculpted in Kreidewachs (chalky wax). Sculpted portions were identified by computed tomography radiography (i.e., CT-scans) (Figure 5A, C, D) provided by the Siemens Magnetic resonance imaging MRT in the Henneberg Klinik in Hildburghausen. Therefore, we know that despite the additions, the length and most other measurements are not heavily altered. A digital photogrammetric 3D-model of the mandible was reconstructed from a series of photos using Reality Capture (RC) and visualized with AVIZO.

Terminology and Comparative Materials

The osteological description follows the terminology of Smuts and Bezuidenhout (1993, 1994) and Göhlich (1998). Measurements of bones and teeth were taken according to Göhlich (1998) using callipers.

For osteological comparisons with other mammutid taxa we considered the descriptions and figures of the following material: skeletal remains of *Z. turicensis* from Mikulov-Czujan's sandpit, Czech Republic (Březina, 2014; Březina and Ivanov, 2015), of *"M". borsoni* from Milia, Greece (Tsoukala, 2000; Tsoukala and Mol, 2016) and from Velenje, Slovenia (Rakovec, 1997), and of the "Warren Mastodon" (*Mammut americanum*) from Newburgh, N.Y. (AMNH 9950) described by Warren (1852) and figured by Olsen (1972). The online 3D-images of the "Buesching Mastodon" (specimen of *Mammut americanum* housed at the Indiana State Museum; ISM 71.3.261) from Fort Wayne, Indiana, provided by the UMORF Bone-Picker (https://umorf.ummp.lsa.umich.edu/wp/vertebrate-2/mammutidae/) were very helpful.
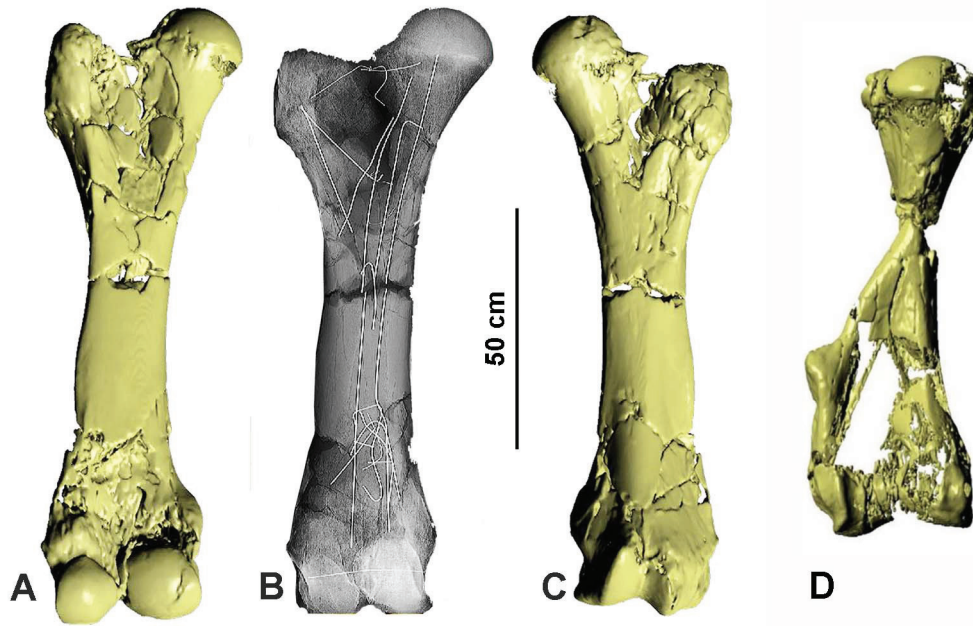
FIGURE 5. Preservation and restoration of *"Mammut" borsoni* long bones from Kaltensundheim: 3D models based on CT scans of the left femur (NHMS-MTe 810/4) (**A:** caudal, **C:** cranial) and left humerus (NHMS-MTe 810/2) from caudal (**D**). After subtracting the (low density) glue and added artificial material, the fragmentation of the bones and the state of preservation are evident (A, C, and D). **B:** The x-ray shows the internal stabilization with metallic rods.

Considered European Localities with Mammutidae

For comparison, we considered and partly reinvestigated several mammutid dentitions, especially mandibles, from selected European localities that are listed below with their stratigraphic position in Figure 3.

Zygolophodon turicensis Group

Localities with detailed stratigraphic references:

Marsolan (FR); early Miocene, MN3b, (Tassy, 1985; Mein, 1999)

Artenay (FR); early Miocene, MN4, isolated molars (Tassy, 1977)

Puente de Toledo (ES); MN5 (Mazo and van der Made, 2012)

Pontlevoy (FR); middle Miocene, MN5 (Tassy, 1985)

Klein-Hadersdorf (AT); middle Miocene, MN6, molars (Schlesinger, 1917; Harzhauser et al., 2011)

Devínská Nová Ves (Neudorf a.d. March) (SK); middle Miocene, MN6, coll. SNM, NHMW (Tóth, 2010a, 2010b; Zapfe, 1954)

Mikulov-Czujan's sandpit (CZ); middle Miocene, MN6, teeth, shortened mandibles without tusks as well as some with tusks alveoli, postcranial bones, coll. MZM, PIUW, RMM (Březina, 2014; Březina and Ivanov, 2015; Březina et al., 2021).

Elgg (CH); middle Miocene, MN6-7; type specimen of *Z. turicensis:* m2 sin, coll. PIMUZ, (Hünermann, 1983)

Rajégats (Simorre, FR); middle Miocene, MN6-7 (Tassy, 1985)

Malartic (Gers, FR); middle Miocene, MN7 (Tassy, 1977, 1985)

Freising (Bavaria, DE); middle Miocene, MN6-7/8, coll. BSPG destroyed in in WW II) mandible with lower tusks and a moderately extended symphysis (Lehmann, 1950)

Tutzing (Bavaria, DE); middle Miocene MN6-7/8, coll. BSPG destroyed in in WW II); mandible with lower tusks and a moderately extended symphysis (Lehmann, 1950).

Villefranche d'Astarac (Gers, FR); middle Miocene, MN7+8), skull and mandible with long (but extensively reconstructed) mandibular symphysis and lower tusks, coll. currently MNHN (Pontier, 1926; Tassy, 1985; Duranthon et al., 1995).

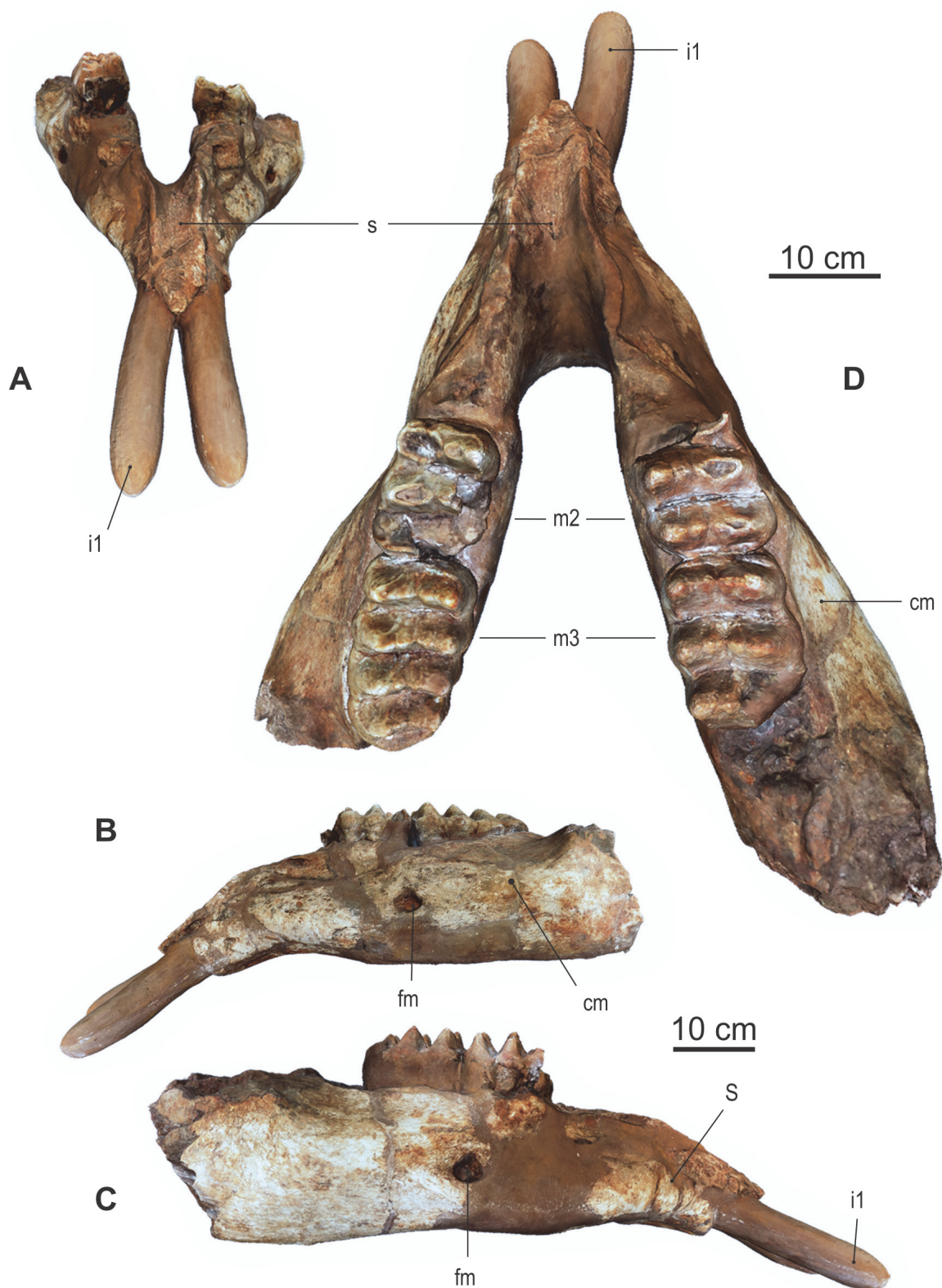**FIGURE 6.** Mandible of *"Mammut" borsoni* from Kaltensundheim (NHMS-MTe 810/1). **A:** Anterior aspect of the symphysis, note that the rami are slightly distorted (not to scale due to perspective view). **B:** Left ramus from buccal. **C:** Right ramus from buccal. **D:** Occlusal aspect of the dentition and the mandible. **Abbreviations:** cm – corpus mandibulae, fm – foramen mandibulae, i1 – mandibular tusk, s – symphysis.

Wolkersdorf - Rochusberg (AT); late Miocene, MN9-11 (Harzhauser et al., 2004); incomplete mandible with a short symphysis but no lower tusks, coll NHMW, 1981/86/1, own investigation.

Soblay (Ain, FR), late Miocene, MN10 (Lortet and Chantre, 1878; Tassy, 1985)

"Mammut" borsoni Group

Within the *"M". borsoni* group, we summarize localities with evidences of *"M". borsoni* and some other related European specimens from the upper Miocene of uncertain taxonomic status.

Localities with detailed stratigraphic references:

Cerro de la Garita (Concud, ES); late Miocene, MN12 (Adrover, 1962, 1963; Mazo and van der Made, 2012)

La Basilla (Valencia, ES); late Miocene, MN 11 (Mazo and van der Made, 2012)

Las Pedrizas (Concud 2, ES); late Miocene, MN12 (Adrover, 1962, 1963; Mazo and van der Made, 2012)

Valdecebro 2 (ES); late Miocene, MN13 (Mazo, 1981; Mazo and van der Made, 2012)

Belka (Odessa region, UA); middle Miocene, MN12, *"Turicius turicensis"* (= *"M". borsoni)* (Krakhmalnaya, 2008; Konidaris and Koufos, 2013)

Pikermi (GR); late Miocene, MN12, juvenile mandibles and skull (Tassy, 1985; Markov, 2008)

Samos (GR); late Miocene, MN12, (Konidaris and Koufos, 2009)

Neokaisaria (GR); middle Miocene, MN12, partial skeleton (Konidaris and Tsoukala, 2020)

Ahmatovo (BUL); Turolian, MN11-MN13, mandible, *"M". obliquelophus* (Nikolov and Kovačev, 1966; Markov, 2004, 2008)

Husnicioara Coal pit (RO); MN14, left m2 (Codrea and Diaconu, 2007)

Otman Hill (Colibaşi, MDA); MN15, partial skull (Obada, 2014)

Alt-Lichtenwarth (= Große Thorstätten, Mühlberg, AT); MN14-16, isolated molars, coll. PIUW (Thenius, 1978)

Milia (GR); upper Pliocene, MN15, mandibles and tusks, coll. Grevena (Tsoukala, 2000; Tsoukala and Mol, 2016)

Vialette near Puy en Veley (Haute Loire, FR); Villlafranchian, MN16, mandibles with and without mandibular tusks, coll. ML (Lortet and Chantre, 1878; Lacombat et al., 2008)

Hajnáčka (= Ajnácskő, SK); late Miocene, MN16, mandible with short symphysis and isolated molars, coll. HNHM, SNM (Schlesinger, 1922; Fejfar, 1961, 1964; Ábelová, 2003; Tóth, 2010a)

Kuzmice (SK); Pliocene, MN16/17, Maxilla with M3, (Černaňský, 2006)

Kaltensundheim (DE); MN16/17, partial skeleton, coll. NHMS (this paper)

Nová Vieska (SK); MN17, isolated molars, coll. SNM (Holec, 1996; Tóth, 2010a, 2010b)

Strekov (SK); MN17, isolated molars, coll. SNM (Holec, 1996; Tóth, 2010a, 2010b)

Localities without detailed stratigraphic references:

Balta (Podolia district, UA); middle Miocene, Cranium and lower jaw of *"M". praetypicum,* coll. ISEA-Krakow (Kubiak, 1972)

Bernhardsthal (AT); Miocene/Pliocene, molars, coll NHMW, PIUW (own investigation)

Bosilkovtsi (Ruse district, north BUL); Plio-/Pleistocene, (Chalwadžiev, 1986)

D'Autrey (Haute Saône, FR); Pliocene, coll. MD (Bergouinoux and Crouzel, 1961)

Farladani (= Ferladany, Fîrlădeni, MDA); Miocene/ Pliocene, mandible (Pavlow, 1894)

Fauverney, Mas-De-Marmote (Cote d'Or, FR); Pliocene, mandible without tusks, coll ML (Lortet and Chantre, 1878)

Nikolajew (=Mykolajiw, UA); Miocene/Pliocene, partial skeleton (Brandt, 1860; Pavlow, 1894)

Pestchana (Podolia, UA); Miocene/Pliocene, mandible without tusks (Pavlow, 1894)

Romanovka (UA); Miocene/Pliocene, type-mandible of *"M". obliquelophus,* coll. OSUM (Mucha, 1980)

Škale near Velenje (SVN); lower Villafranchian, Carpalia (Rakovec, 1997).

Szabadka (Bács-Bodrog, HU); Pliocene, isolated molars (Schlesinger, 1922)

Villanova d'Asti (Piemont, IT); Pliocene, Villafanchian, M3 sup., type material of *"M". borsoni* (Hays, 1834; Osborn, 1936; Masini and Sala, 2007).

Abbreviations

BSPG Bayerische Staatsammlung für Paläontologie und Geologie München in Staatli-

che Naturwissenschaftliche
Sammlungen Bayerns, München (DE)

HNHM Hungarian Natural History Museum,
Budapest (HU)

ISEA Institute of Systematics and Evolution of
Animals, Krakow (PO)

MD Muséum d'Histoire Naturelle, Dijon (FR)

ML Musée des Confluences, Lyon (FR)

MZM Moravian Museum, Brno (CZ)

NHMS Naturhistorisches Museum Schleusin-
gen, Thuringia (DE)

NHMW Naturhistorisches Museum Wien (AT)

OSUM Odessa State University Museum
Odessa (UA)

PIUW Paläontologisches Institut der Universi-
tät Wien (AT)

PIMUZ Paläontologisches Institut und Museum
der Universität Zürich (CH)

RMM Regional Museum in Mikulov (CZ)

SFQW Senckenberg Forschungsstation für
Quartärpaläontologie Weimar (DE)

SNM Slovak National Museum, Bratislava (SK)

SNSB Staatliche Naturwissenschaftliche Sam-
mlungen Bayerns (DE)

For countries the international codes are used: AT
– Austria; BUL – Bulgaria; CH – Switzer-
land; CZ – Czech Republic; DE – Ger-
many; ES – Spain; FR – France; GR –
Greece; HU – Hungary, MDA – Moldova;
PO – Poland; RO – Romania; SK – Slo-
vakia; SVN – Slovenia; UA – Ukraine.

SYSTEMATIC PALEONTOLOGY

Proboscidea Illiger, 1811
Elephantiformes Tassy, 1988
Elephantimorpha Tassy and Shoshani, 1996
Mammutidae Hay, 1922
Mammut Blumenbach, 1799
"Mammut" borsoni (Hays, 1834)
(Figures 5-15)

Mandible and its Dentition

The mandible (NHMS-MTe 810/1) (Figures 4
and 6, Table 1) comprises both corpora mandibu-
lae with left and right m2 and m3 and the symphy-
sis, but both ascending rami are broken off. In front
of the m2 the bone surface is rough indicating the
closed alveoli of the shed m1. The fragmented jaw
was restored. On a historical photo (Figure 4A) the
individual fragments can be recognized easily. In
the restored jaw, the tooth rows are moderately
converging mesially, and the left hemimandible is
slightly twisted, but this is probably due to the
reconstruction. The lower margin of the mandible is
almost straight and slightly ventrally inclined at the
symphyseal angle. The preserved symphysis is 24
cm long and holds two small lower tusks. The ante-
rior-most portion of the symphysisis incomplete;
thus, the complete symphysis might have been
slightly longer. On both sides, a large foramen
mentale opens laterally on the corpus mandibulae
below the distal end of the m2 at about 38 cm from
the preserved tip of the symphysis.

Tusks. The actual state of the lower tusks in the
Kaltensundheim mandible is reconstructed by plas-
ter (Figure 6). Details of the original tusks, how-
ever, are documented in photos (Figure 4 A and B).
Their diameter is about 5 cm according to the size
of the alveoli, and their reconstructed external
length is about 15 cm, which corresponds to what
is seen on the photos. According to this picture, the
reconstruction is accurate. The current where-
abouts of the original lower tusks is unknown.

No upper tusks were associated with this indi-
vidual. However, the second individual from the
same sinkhole, housed in Weimar (SFQW), exhib-
its fairly straight tusks, about 1.5 m long (Figure 2).
The precise orientation of these tusks is straight or
slightly curved upwards, and resemble the upper
tusks from Milia (Touskala and Mol, 2016). It is
likely that there is some variability in this character.
Important for the differentiation of *"M". borsoni* from
Z. turicensis is the lack of an enamel band on the
upper tusk. No traces of an enamel band are pres-
ent on the upper tusk of the second individual

TABLE 1. Measurements (mm) of the mandible of *"Mammut" borsoni* from Kaltensundheim.

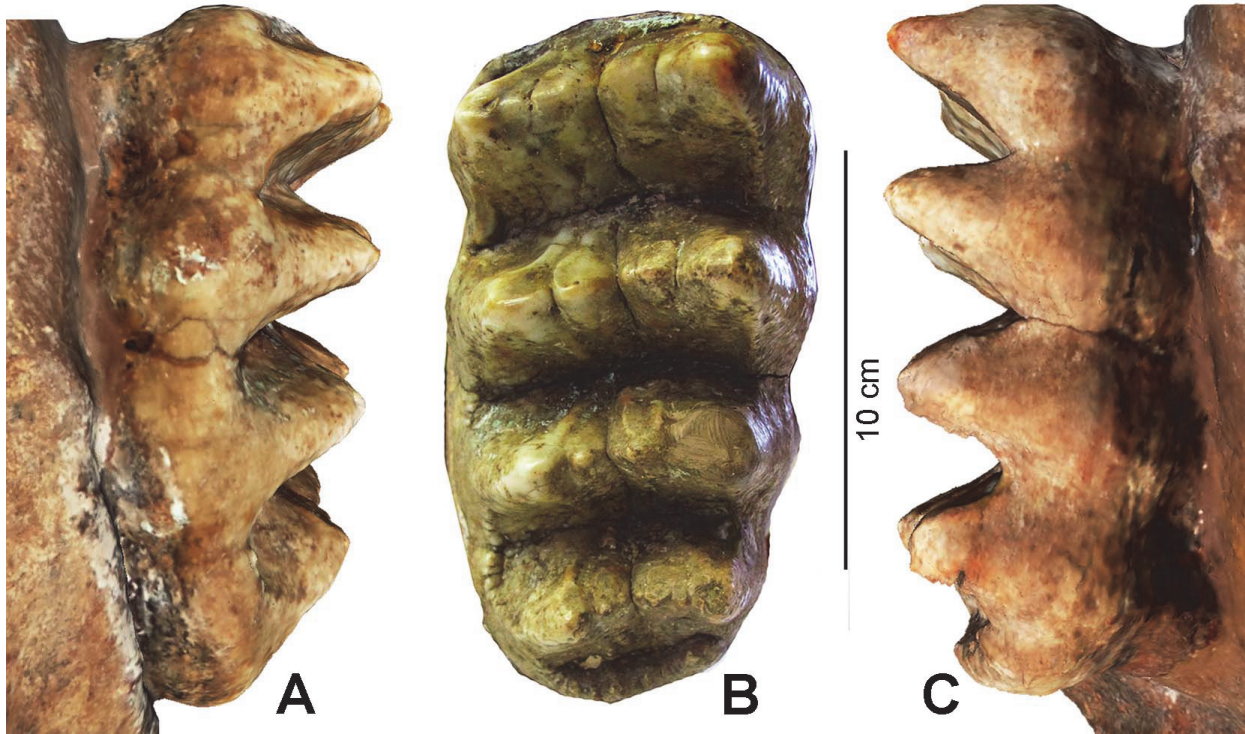| mandible (1)	mm
length of preserved symphysis (slightly incomplete)	240
height of corpus mandibulae below posterior end of m3	160
height of corpus mandibulae at level of foramen mentale	150
height of symphysis at symphyseal angle	180
min. width of symphysis	120

FIGURE 7. Left m3 of *"Mammut" borsoni* from Kaltensundheim. **A:** buccal (pretrite), **B:** occlusal, **C:** lingual (posttrite); B photo, A and C from 3D reconstruction.

(pers. comm., W.-D. Kahlke, Sept. 2019). The same can be assumed for the decribed specimen.
Molars. When this individual died, m2 and m3 were in occlusal wear on both sides (Figures 6 and 7, Table 2). In front of both m2 the bone surface is rough indicating the closed alveoli of the shed m1. The molars on the left side are worn slightly more than the right ones. Such minor asymmetry in occlusal wear reflects the individual mode of mastication and occurs frequently in mammalian dentitions.

Both m2 are moderately worn and partly broken. The right m2 lacks the entire first lophid, while the crown of the posterior lophid on the left m2 is missing. The m2 are trilophodont with a zygodont pattern. The lophids are sharp-crested and the valleys are unblocked without any conules. The

median sulcus is distinct, but shallow. The pretrite (buccal) half-lophids are all worn down to the dentine. A main cusp and one mesoconelet make up the posttrite half-lophids. The mesoconelet is lower but of similar width like the main cusp. Zygodont crests are present on all posttrite half-lophids, stronger on the posterior slope than on the anterior one. On the left m2, the facet of the second pretrite half-lophid shows a small anterior trefoil; a residual cingulum is present in the labial exit of the first pretrite valley. Narrow and low cingula are present on the anterior and the posterior end.

Both m3 are well preserved (Figure 7) and only slightly worn on the anterior slopes and tips of the first and second lophid. The left m3 is complete, the right one is missing the forth lophid and the pretrite third half-lophid. The m3 is made up by

TABLE 2. Measurements (mm) of the molar dentition of *"Mammut" borsoni* from Kaltensundheim.

molars	length	max width	W-1	W-2	W-3	W-4	height
m2 sin	105	84	73	~80	~84	-	-
m2 dext	-	-	-	80	83		-
m3 sin	164	90	83	90	86	77	54 (2nd)
m3 dext	-	-	82	88	-	-	57 (2nd)
m2 + m3	267	-					

four zygodont lophids and a low and crenelated posterior cingulum, which is slightly shifted to the lingual side. The posterior slopes of the lophids are slightly concave and steeper than the anterior ones. All valleys are totally open and not blocked by any conules. The median sulcus is distinct but shallow, and weaker in the posterior lophids. The pretrite half-lophids consist of a main cone and one mesoconelet, whereas the posttrite half-lophids show two to three somewhat irregular mesoconelets. The pretrite half-lophids are slightly broader and higher than the posttrite ones. All posttrite main cones have zygodont crests. A crenelated labial cingulum is present in all pretrite exits of the valleys. On the anterior slopes of all pretrite main cusps a bulge of enamel runs down in median direction, crossing the mesoconelet. This is important, because during mastication, the first clear facet is formed on this anterior structure of each loph.

Molar wear facets inform mastication movements in *"M". borsoni.* The lower jaw is lifted in an almost orthal direction during phase I of the chewing cycle, so that the lophids of the lower and the lophs of the upper molars intercalate. The facets on the pretrite half-lophids in the lower molars indicate that the movement is not exactly in an orthal direction but creates some pressure in an anterior direction. Accordingly, food items are compressed against the steep posterior slope of the lophids without forming a distinct facet. The anterior facets are only visible as long as no dentine is exposed. Such facets were observed in several other dentitions of *Zygolophodon*, but in *M. americanum* are less common (Tassy, 2014, Koenigswald, 2016). Phase II of the chewing cycle could not be identified in *"M". borsoni*, but a lateral movement in lingual direction as seen in juvenile teeth of *M. americanum* cannot be excluded (Laub, 1996).

When the teeth are abraded to such a degree that the dentine is broadly exposed, the surrounding enamel forms a functional ridge, across which food items are pressed. This requires some lateral movement. In the Kaltensundheim specimen, the fragmentary m2 show the classic difference in wear between the pretrite and posttrite sides. It is caused by the different duration of the contact between upper and lower tooth rows. In the acting side, the lower molars move to the lingual side. Therefore, during each chewing cycle the pretrite sides buccal on the lower and lingual on the upper molars are occlude for a longer stroke than the postrite sides. Thus, more intensive abrasion on the pretrite sides marks the longer contact between

the antagonists. The prerequisite of such a lateral movement is the alternating occlusion of the right and left tooth rows (Laub, 1996; Koenigswald, 2016). The pretrite-postrite difference in wear occurs in gomphothere dentitions as well, whereas in Elephantidae both sides probably occlude simultaneously and chew in proal direction.

Postcranial Elements

The postcranial material is catalogued as NHMS-MTe 810/2-37. For space-saving reasons only the last number is indicated (in brackets) in the following text. The osteological comparative material of other mammutid taxa is listed above in the section Materials and Methods.

Forelimbs

Scapula. The material at the NHMS includes a small fragment of the scapula (17). Preserved is a small centerpiece of the scapula with the distal base of the broken spina scapula, but allows no further description or measurements.

Humerus. The right humerus (6) (Figure 5D and 8, Table 3) is almost complete but lacks the crista supracondylaris lateralis. The left humerus is more fragmentary, missing the crista lateralis and the central part of the distal diaphysis. According to the CT-scans of the left humerus, the shape of the crista surpracondylaris and the full length of the bone is accurate. In both humeri, the proximal epiphyses are fused, but the sutures are still visible. The spherical caput humeri is slightly compressed mediolaterally. In proximal view, the tuberculum major projects significantly cranially and is separated from the caput by a deep sulcus intertubercularis. The medial outline of the humerus is distinctly convex. The mid-shaft is of triangular shape with concave lateral and caudal surface. Along the lateral surface of shaft twists a wide and slightly concave sulcus musculi branchialis. The crista supracondylaris lateralis is widely projecting laterally forming a prominent wing and ends in a distinctive salient angle. This prominent wing extends about the distal 2/5 of the entire length of the humerus. The result is that the distal half of the humerus is distinctly wider than the proximal half. The crista humeri continues distally as a ridge down to the trochlea by crossing vertically the cranial fossa radialis. The trochlea humeri is separated by a shallow sagittal sulcus in a wider medial portion and a less wide lateral portion. In distal view, this sagittal sulcus is deeper caudally (in the proximity of fossa olecrani) than cranially. The craniocaudal depth of the trochlea humeris is
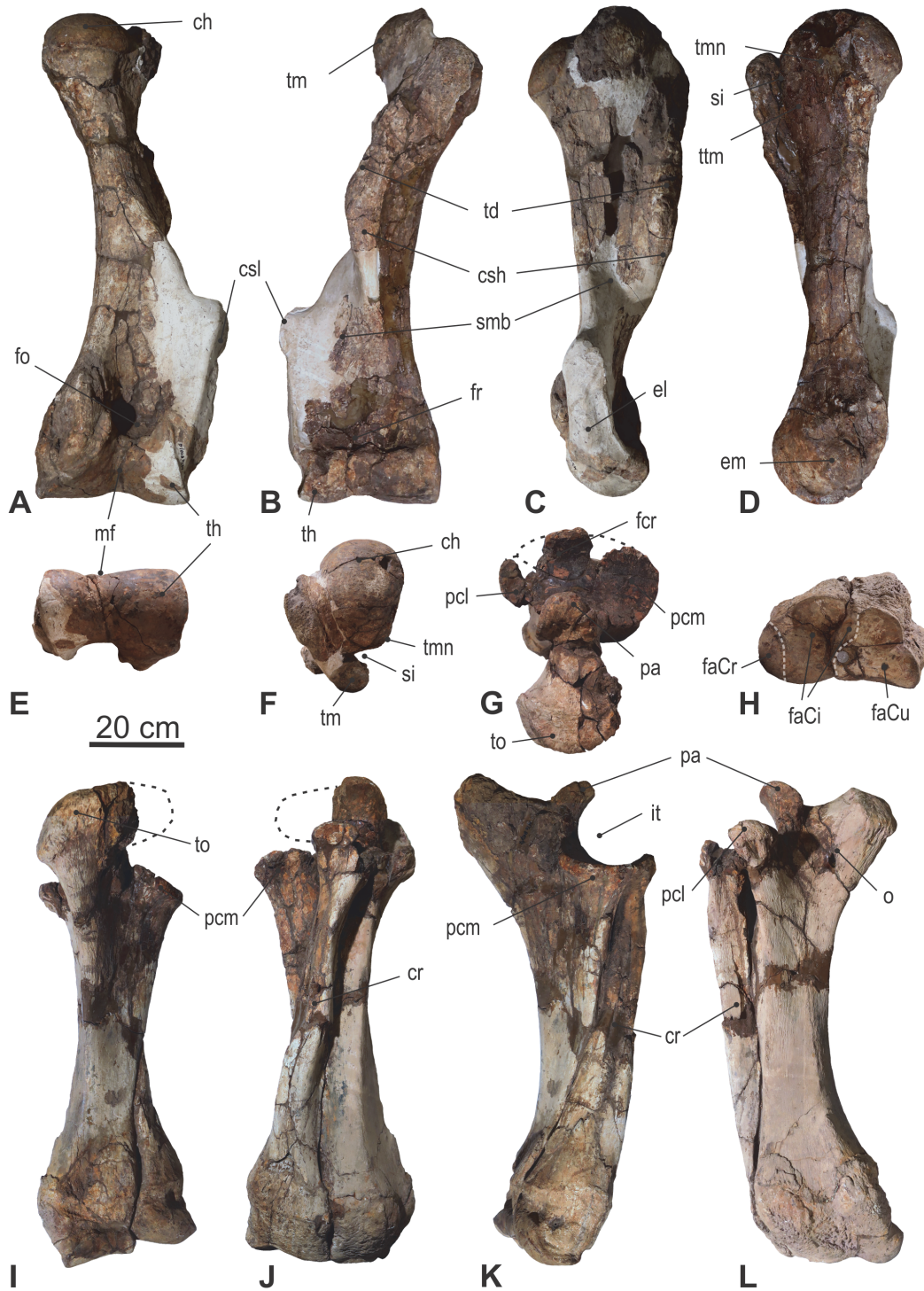
FIGURE 8. Long bones of the forelimb of *"Mammut" borsoni* from Kaltensundheim. **A-F:** humerus dext (NHMS-MTe 810/6), **G-L:** radius and ulna sin in articulation (NHMS-MTe 810/7). A – caudal, B – cranial, C and L – lateral, D and K – medial, F and G – proximal, E and H – distal, I – palmar, J – dorsal. **Abbreviations:** Humerus: ch – caput humeri, csh – crista humeri, csl – crista supracondylaris lateralis, el – epicondylus lateralis, em – epicondylus medialis, fo – fossa olecrani, fr – fossa radialis, mf – median furrow, si – sulcus intertubercularis, smb – sulcus musculus brachialis, td – tuberositas deltioidea, th – trochlea humeri, tmj – tuberculum majus, tmn – tuberculum minus, ttm – tuberositas teres minor. **Radius:** cr – corpus radii, faCi – facies articularis carpea for Ci, faCr – facies articularis carpea for Cr, fcr – fovea capitis radii. Ulna: faCu – facies articularis carpea for Cu, it – incisura trochlearis, o – olecranon, pa – processus anconeus, pcl – processus coronoideus lateralis, pcm – processus coronoideus medialis, to – tuber olecrani.

TABLE 3. Measurements (cm) of the long bones of *"Mammut" borsoni* from Kaltensundheim (measurements taken according to Göhlich, 1998). **Abbreviations:** Cdia – circumference of diaphysis, Dcap – depth of caput femoris, Dd – distal depth, Ddia – depth of diaphysis, Dolec – depth of olecranon from proc. anconaeus, Dp – proximal depth, Dtr – depth of trochlea, GL – greatest length, GLc – greatest length incl. caput, GLmed – greatest length medially, GLtroch – greatest length incl. trochanter, Lcrepi – length of crista epicondyluslateralis, Li – length of incisura trochlearis, Llat – greatest length laterally, Lph – physiological length, Wcap – width of caput femoris, Wd – distal width, Wdia – width of diaphysis, Wdtr – width of distal trochlea, Wolec – width of olecranon, Wp – proximal width.

	Hum dext	Hum sin	Rad dext	Rad sin	Ulna dext	Ulna sin	Fem dext	Fem sin	Tib dext	Tib sin	Fib sin
GL	107	~101	~77	79	89	92	125	127	80	85	~77
Lph	97	100	-	73	74	76	119	123	-	74	-
GLc	98	101	-	-	-	-	-	-	-	-	-
GLtroch	-	-	-	-	-	-	119	-	-	-	-
Llat	-	-	-	-	-	-	-	117	-	-	-
GLmed	-	-	-	-	-	-	-	-	77	-	-
Wp	30	~28	-	11.5	-	30	-	19	30	31	-
Wcap	-	-	-	-	-	-	20.5	-	-	-	-
Dcap	-	-	-	-	-	-	19.5	-	-	-	-
Dp	34.5	36.5	-	9	-	-	-	19	-	~22	-
Li	-	-	-	-	-	16	-	-	-	-	-
Wolec	-	-	-	-	-	~19	-	-	-	-	-
Dolec	-	-	-	-	40	-	-	-	-	-	-
Wdia	13	-	4	5	-	-	18	18	12.5	13	2.5
Ddia	-	~14	-	7	-	-	10.5	10	12	10	3.8
Cdia	52.5	~41	-	21	25	-	46.5	47	39	39	16
Wdtr	28	30	-	-	15.5	15	27	21	21	-	-
Wd	-	34	13	12	~20	-	28.5	31	-	22	11.5
Dd	-	~20.5	17	20	-	-	-	-	17.5	17	15
Lcrepi	-	40	-	-	-	-	-	-	-	-	-
Dtr	-	-	-	-	14	14	29	29	-	-	-

almost the same in the medial and lateral part. The caudal fossa olecrani is small but deeply excavated.

The extended and angular proximal end of the crista supracondylaris lateralis is typical for Mammutidae and less pronounced in other proboscideans. The proximal half of the humerus of the Kaltensundheim specimen is in craniocaudal aspect slenderer than that of *M. americanum* due to the weaker crista humeri. The distal end of the Kaltensundheim humerus is angled slightly cranially (compared to the shaft); as a result, the crista supracondylaris lateralis is only slightly inclined caudally compared to the axis of the shaft. The cranial deflection of the distal humerus and the caudal inclination of the crista supracondylaris is more pronounced in *M. americanum*. In this character the Kaltensundheim humerus is similar to *Z. turicensis*. The humeral trochlea of the Kaltensundheim specimen and in *Z. turicensis* are relatively wide (ratio width/depth of trochlea in Kaltensundheim 1.46, in *Z. turicensis*, 1.57). This ratio varies in the three humeri from Milia (Tsoukala and Mol, 2016, tab. 10) between 1.12 and 1.37 in comparison to 1.3 in *M. americanum*. In general, the ratio may be somewhat lower in *"M". borsoni*, but the taxonomic value of this character remains uncertain.

The median sulcus of the trochlea is narrower in the Kaltensundheim humeri than in *M. americanum*. A peculiarity in the Kaltensundheim specimen seems to be the vertical ridge intersecting the cranial fossa radialis, which is observed neither in *Z. turicensis* nor in *M. americanum*. In proximal view, the tuberculum major is mediolaterally less massive than in *M. americanum*.

Radius and Ulna. Both right and left radius and ulna (Figure 8, Table 3) are preserved in articulation, but if they are fused by ossification or preparation is unclear. The distal epiphysal sutures of ulna

and radius are closed, but still visible. A small spatium interosseum antebrachii is visible only between the proximal fourth of the shaft of radius and ulna.

Right (3b) and left (7b) radius are almost complete, but both lack the lateral portion of the proximal epiphysis. The left radius is the best preserved. The proximal articular facet of the radius is dorsopalmarly concave, supporting the rotation of the humerus. Its lateral part is missing, but according to the lateral processus coronoideus of the ulna its shape was triangular. The palmar articular facets on the proximal end of the radius for the ulna are not visible. The radius twists around the dorsal side of the ulna and articulates to its medial distal end. The shaft of the radius is slender and thickens in its distal third. Both distal facets, for the radiale (scaphoideum) and the intermedium (lunatum) are convex and separated by a dorsopalmarly convex bulge. In distal view, the distal ends of radius and ulna are of similar size and the contact-line to the ulna is concave. The dorsolateral edge of the distal facet for the intermedium forms a triangular extension and is concave in profile.

Both ulnae (7 sin, 3a dext) are well preserved, in the right one, only the tip of the processus anconaeus and the lateral part of the processus coronoideus is missing; in the left one, the medial portion of the olecranon is broken off.

The olecranon is very robust and extends laterally. The processus anconaeus is shifted slightly to the lateral side and points proximodorsally; it reaches about the same height as the olecranon, from which it is separated by a clear concave indentation. A distinct protuberance covers the proximal side of the processus anconaeus and widens the processus to both sides.

In proximal view, the medial processus coronoideus is twice as large as the lateral one and carries an almost circular facet whereas the facet on the lateral process is more irregular. The shaft narrows towards the midshaft and is triangular in cross section with all three surfaces almost concave. The distal end of the ulna is deeper than wide, angular, and not rounded. The ulna articulates distally with a small part of the intermedium (lunatum) and the radiale (scaphoideum). The facet for the intermedium is strongly inclined towards the radius and separated by a crest from the facet to the radiale. The latter facet is almost triangular, dorsally concave, and palmarly convex. The palmar sides of ulna and radius show deep depressions proximal to the distal articulation.

On the distal radius, the edge between the both distal articulation facets is rounded in the Kaltensundheim *"M". borsoni*, whereas it is distinctly sharper in *Z. turicensis*. The distal articular facets on the radius and ulna cover almost the entire distal side of the bones in the Kaltensundheim *"M". borsoni* and in *M. americanum*, whereas in *Z. turicensis* the facets are relatively smaller. The extended facets in *"M". borsoni* and *M. americanum* allow a wider rotation in dorsal direction. The proximal margin between olecranon and processus anconaeus forms a deep indentation in the Kaltensundheim specimen, whereas the margin is almost straight in *Z. turicensis* and *M. americanum*. The distal contact between ulna and radius is slightly medially convex in the Kaltensundheim specimen and in *M. americanum*, but is almost straight in *Z. turicensis*.

Manus

The skeleton of the hand in Mammutidae contains the same elements as in Elephantida. The bones, however, differ slightly in their articulation. We mention below the observed differences between *Z. turicensis*, *"M". borsoni*, and *M. americanum*, but because of the limited material, the individual variability within each taxon cannot be fully evaluated. The carpal elements of *"M". borsoni* from Milia would be of interest because of the differences in body size, but they are not described in detail, so far. Measurements of the carpal and metacarpal bones according to Dubrovo and Jakubowski (1988) and Göhlich (1998) are provided in Tables 4-6.

Carpalia

All four bones of the proximal row of carpalia are preserved (Figures. 9, 10, 11, 12, Tables 4 and 5): os carpi radiale (Cr = scaphoideum), os carpi intermedium (Ci = lunatum), os carpi ulnare (Cu = cuneiforme), and os carpi accessorium (Ca = pisiforme). All stem from the left hand, except for the Cu, which comes from the right hand.

The ulna articulates mostly with the Cu, but also with Ca and marginally with Ci in a saddle shape facet, and the radius articulates predominately with the Ci and a smaller oval facet of Cr (see Figure 10). The combined proximal facets for the ulna and the radius are of similar size. The combined proximal facet for the radius is in large parts dorsopalmarly concave, only in its dorsomedial portion its surface is convex. The combined facet for the ulna is predominantly concave,

TABLE 4. Measurements (mm) of the proximal row of carpal bones of *"Mammut" borsoni* from Kaltensundheim (measurements according to Göhlich, 1998). Indicated in square brackets is/are the bone/s to which the facet articulates. **Abbreviations:** DdFl – depth of dist. lateral facet [for Cu], DdFm – depth of dist. medial facet [for Cr, or Ci], Ddg – max. depth of Cu diagonal, DFd – depth of dist. facet [for CI-CIII, or CII-IV, or CIV], DFdl –depth of distolateral facet [for McV], DFl – depth of lateral facet [for Ci], dFl – minimal distance between lateral facets, dFm – minimal distance between medial facets, DFp – depth of proximal facet [for Ci, Rad., or Ulna], DpFl – depth of prox. lateral facet [for Cu], DpFm – depth of prox. medial facet [for Cr, or Ci], GD – greatest depth, GH – greatest height, GW – greatest width, HdFl – height of dist. lateral facet [for Cu], HdFm – height of dist. medial facet [for Cr, or Ci], HFdl – depth of distolateral facet for [McV], HFl – height of lateral facet [for Ci], HFpa – height of palmar facet [for Ca], HFpdo – width of proximodorsal facet [for Cu], Hm – medial height, HpFl – height of prox. lateral facet [for Cu], HpFm – height of prox. medial facet [for Cr, or Ci], WD – min. width of "diaphysis", Wd – distal width, WFd – width of dist. facets [for CI-CIII, CII-IV, or CIV], WFp – width of the proximal facet [for Ci, Rad., or Ulna], WFpa – width of palmar facet [for Ca], WFpdo – width of proximodorsal facet [for Cu], Wp – proximal width.

Cr = Os carpi radiale (scaphoideum)		Ci = Os carpi intermedium (lunatum)		Cu = Os carpi ulnare (cuneiforme)		Ca = Os carpi accessorium (pisiforme)	
GH	138	GH	99	GH	106	GH	172
GD	139	GD	166	GD	135	GD	76
GW	87	GW	144	GW	171	WD	63
-	-	-	-	Ddg	202	Wp	86
-	-	-	-	Hm	70	Wd	89
WFp [Ci]	31	WFp [Rad.]	131	WFp [Ulna]	143	WFp [Ulna]	80
DFp [Ci]	86	DFp [Rad.]	136	DFp [Ulna]	110	DFp [Ulna]	34
WFp [Rad.]	50	-	-	WFpa [Ca]	56	WFpdo [Cu]	86
DFp [Rad.]	90	-	-	HFpa [Ca]	24	HFpdo [Cu]	52
WFd [CI-CIII]	67	WFd [CII-IV]	139	WFd [CIV]	159	-	-
DFd [CI-CIII]	95	DFd [CII-IV]	129	DFd [CIV]	120	-	-
DFl [Ci]	87	DpFl [Cu]	60	DFdl [McV]	107	-	-
HFl [Ci]	28	HpFl [Cu]	45	HFdl [McV]	64	-	-
-	-	DdFl [Cu]	101	-	-	-	-
-	-	HdFl [Cu]	35	-	-	-	-
-	-	DpFm [Cr]	86	DpFm [Ci]	40	-	-
-	-	HpFm [Cr]	39	HpFm [Ci]	15	-	-
-	-	DdFm [Cr]	87	DdFm [Ci]	60	-	-
-	-	HdFm [Cr]	25	HdFm [Ci]	25	-	-
dFl	22	-	-	dFm	14	-	-

becomes almost flat dorsomedially before it bends onto the Ci.

The radiale (Cr, scaphoideum) (21) (Figure 11A-F, Table 4) tapers in a proximal direction. Its medial surface is rough and irregular. The proximal facet for the radius is elliptical, slightly concave, and laterally inclined. The adjacent lateral facet for the intermedium (Ci) is oriented vertically, semicircular in shape and lowering dorsally. These two facets form an almost perpendicular angle. A second facet for the intermedium is situated distally on the lateral side and forms a low, longitudinal band, descending in dorsal direction. The distal articular facet for the CII is triangular, slightly convex, and shifted dorsally on the distal end.

Compared to the Kaltensundheim specimen, the proximal facet for the radius is steeper and inclined laterally in *M. americanum.* Also, the distal facet for the second carpal is relatively small covering a smaller part of the distal end and is oriented almost horizontally (more inclined laterally in Kaltensundheim specimen), the palmar tuberosity is more bulging and inflated, and the dorsopalmar extension for both lateral facets for the intermedium are dorsopalmarely shorter and more distant to each other. No radiale of *Z. turicensis* is known.

The overall shape of the intermedium (Ci, lunatum) (20) (Figure 11G-L, Table 4) is triangular in proximal view, widening dorsally. Due to the concave proximal and distal surfaces, the bone is lowest in the middle. The palmar end forms a

TABLE 5. Measurements (mm) of the distal carpal bones of *"Mammut" borsoni* from Kaltensundheim (measurements according to Göhlich, 1998). Indicated in square brackets is/are the bone/s to which the facet articulates. **Abbreviations:** DdFl – depth of dist. lateral facet [for CIV], DdFm – depth of dist. medial [for CIII], Ddg – diagonal depth, DFd – depth of distal facet [for McI, II, III or IV], DFld – depth of laterodistal facet [for McII], DFl – depth of lateral facet [for CII, CIII], DFm – depth of medial facet [for CI, or CII], DFp – depth of proximal facet [for Cr, Cr+Ci, Ci+Cr+Cu, or Cu], DlFd – depth of lat. distal facet [for McV], DmFd – depth of med. distal facet [for McII, or III], DpFl – depth of prox. lateral facet [for CIV], DpFm – depth of medial facet [for CIII], GD – greatest depth, GH – greatest height, GW – greatest width, HdFl – height of dist. lateral facet [for CIV], HdFm – height of dist. medial facet [for CIII], Hdo – dorsal height, HdoFl – dorsal height of lateral facet [for CIII], HdoFm – dorsal height of medial facet [for CII], HFl – height of lateral facet [for CII], HFld – height of laterodistal facet [for McII], HFm – height of medial facet [for CI], HpaFl – palmar height of lateral facet [for CIII], HpaFm – palmar height of medial facet [for CII], HpFl – height of prox. lateral facet [for ClV], HpFm – height of prox. medial facet [for CIII], minHpFl – minimal height of prox. lateral facet [for ClV], minHpFm – minimal height of prox. medial facet [for CIII], Wdo – dorsal width, WFd – width of distal facet [for McI, II, III or IV], WFp – width of proximal facet [for Cr, Cr+Ci, Ci+Cr+Cu, or Cu], WlFd – width of med. distal facet [for McV], WmFd – width of med. distal facet [for McII, or III], Wpa – palmar width.

CI - Os carpale primum (trapezium)		CII - Os carpale secundum (trapezoideum)		CIII – Os carpale tertium (magnum)		CIV - Os carpale quartum (unciforme)	
GH	90	GH	69	GH	113	GH	125
-	-	-	-	Hdo	89	Hdo	95
GD	101	GD	~120	GD	153	GD	153
GW	61	GW	71	GW	107	GW	136
-	-	-	-	Wpa	105	-	-
-	-	-	-	Wdo	95	Ddg	164
WFp [Cr]	29	WFp [Cr+Ci]	70-80	WFp [Ci+Cr+Cu]	?	WFp [Cu]	135
DFp [Cr]	61	DFp [Cr+Ci]	~110	DFp [Ci+Cr+Cu]	123	DFp [Cu]	126
WFd [McI]	53	WFd [McII]	59	WFd [McIII]	59	WFd [McIV]	86
DFd [McI]	87	DFd [McII]	~105	DFd [McIII]	118	DFd [McIV]	114
-	-	-	-	WmFd [McII]	43	WmFd [McIII]	40
-	-	-	-	DmFd [McII]	111	DmFd [McIII]	117
-	-	-	-	-	-	WlFd [McV]	57
-	-	HpaFl [CIII]	43	-	-	DlFd [McV]	106
HFl [CII]	86	HdoFl [CIII]	70	HpFl [CIV]	59	-	-
-	-	-	-	minHpFl [CIV]	33	-	-
DFl [CII]	47	DFl [CIII]	67	DpFl [CIV]	120	-	-
HFld [McII]	32	-	-	HdFl [CIV]	25	-	-
DFld [McII]	33	-	-	DdFl [CIV]	111	-	-
-	-	HFm [CI]	55	HpaFm [CII]	44	HpFm [CIII]	63
-	-	-	-	-	-	minHpFm [CIII]	39
-	-	-	-	HdoFm [CII]	67	DpFm [CIII]	123
-	-	DFm [CI]	71	DFm [CII]	124	HdFm [CIII]	29
-	-	-	-	-	-	DdFm [CIII]	116
GH/GD	88.5 %	GH/GD	~57 %	-	-	GH/GD	81.7 %
GW/GD	60.3 %	GW/GD	~60 %	-	-	GW/GD	88.7 %

thickened spherical tuberosity; the dorsal surface is highest medially and becomes lower laterally. The proximal facet for the radius almost covers the entire proximal surface and is dorsopalmarly concave in its palmar half, and becomes convex towards its dorsomedial angle. In its dorsolateral edge, the proximal surface articulates with the ulna; this facet faces proximolaterally, is oval, and slightly convex. The distal facet also covers the entire distal surface; it is concave in its palmar half and convex in its dorsal half; it articulates primarily with the CIII and only in its mediodorsal angle with the CII. On the medial surface the two vertical facets for the Cr differ in size; the proximal one is

TABLE 6. *"Mammut" borsoni* from Kaltensundheim: measurements (in mm) of metacarpalia (measurements according to Göhlich, 1998). Indicated in square brackets is/are the bone/s to which the facet articulates. **Abbreviations:** CD – least circumference of diaphysis, Dd – max. distal depth, DD – least depth of diaphysis, DFl – depth of lateral facet [for McIII, McIV or McV], DFm – depth of medial facet [for CI, McII, or McIII], DFp – depth of proximal facet [for CI, CII, CIII, or CIV], DlFp – depth of lateral proximal facet [for CIII or CV], DmFp – depth of medial proximal facet [for CII or CIII], Dp – max. proximal depth, GL – greatest length, HFl – height of lateral facet [for McIII, McIV or McV], HFm – height of medial facet [for CI, McII, or McIII], Wd – max. distal width, Wp – max. proximal width, WD – least width of diaphysis, WFp – width of proximal facet [for CI, CII, CIII, or CIV], WlFp – width of lateral proximal facet [for CIII or CV], WmFp – width of medial proximal facet [for CII or CIII], WTr – max width of distal trochlea.

MC I		MC II		MC III		MC IV	
GL	150	GL	194	GL	217	GL	198
Dp	93	Dp	110	Dp	123	Dp	114
Wp	71	Wp	99	Wp	100	Wp	96
WFp [CI]	68	WmFp [CII]	66	WmFp [CIII]	58	WFp [CIV]	86
DFp [CI]	85	DmFp [CII]	100	DmFp [CIII]	116	DFp [CIV]	111
		WlFp [CIII]	36	WlFp [CIV]	50		
		DFlp [CIII]	110	DFlp [CIV]	119		
		DFl [McIII]	36	DFl [McIV]	94	DFl [McV]	92
		HFl [McIII]	100	HFl [McIV]	42	HFl [McV]	53
		DFm [CI]	32	DFm [McII]	45	DFm [McIII]	97
		HFm [CI]	41	HFm [McII]	100	HFm [McIII]	42
WD	50	WD	79	WD	77	WD	76
DD	64	DD	61	DD	59	DD	61
CD	194	CD	217	CD	227	CD	241
Wd	79	Wd	115	Wd	103	Wd	115
Dd	77	Dd	100	Dd	118	Dd	97
WTr	-	WTr	92	WTr	95	WTr	104

extended, whereas the distal one is oval and restricted to the dorsal half of the distal margin. On the lateral side, the facet for the ulna is framed along its distal edge by a narrow and longitudinal facet for the Cu; the two facets are perpendicular to each other. A second facet for the Cu, distally on the lateral side, is sigmoid-shaped and lowering palmarly.

The Ci of *"M". borsoni* from Kaltensundheim and of *M. americanum* are more robust and more angular than in *Z. turicensis*, which has a more trefoil-shaped Ci with rounded angles. The articular facet for the ulna is steeper (facing more laterally) in the Kaltensundheim specimen and in *M. americanum* than in *Z. turicensis*, in which this facet faces more proximolaterally. This probably results from the fact that the dorsal side of the Ci is lowering stronger towards the lateral edge, than in *M. americanum* and *"M". borsoni* from Kaltensundheim. On the lateral side, the proximal facet for the Cu that accompanies the distal margin of the facet for the ulna forms a longitudinally distinct band in the Kaltensundheim *"M". borsoni*, whereas it is only

weakly adumbrated in *Z. turicensis* and not observable in *M. americanum*.

The right ulnare (24) (Cu, cuneiforme) (Figure 11M-R, Table 4) lacks its mediopalmar portion, and both articular facets for the Ci are incomplete. The bone is triangular in proximal view, tapers laterally, and extends into a lateropalmar process. It is highest in its medial half and lowers laterally. The proximal facet for the ulna is concave in its lateral part and dorsomedially almost flat. The distal facet covers almost the entire distal surface; its primary articulation is with the C4. Even if the mediopalmar corner is broken off, a small area of distal articulation with the C3 can be reconstructed based on the proximal facets of the C3. The lateral process exhibits laterodistally a facet for the C5, but it is not clearly separated from the facet for the C4. On the palmar side, the facet for the Ca is large and semicircular and contacts the proximal facet for the ulna in a sharp straight edge. On the medial side, both facets for the Ci are incomplete; the proximal medial facet for the Ci is low but well developed and continualy curves into the proximal facet for the ulna; the distal medial facet is somewhat bigger than the proximal one.
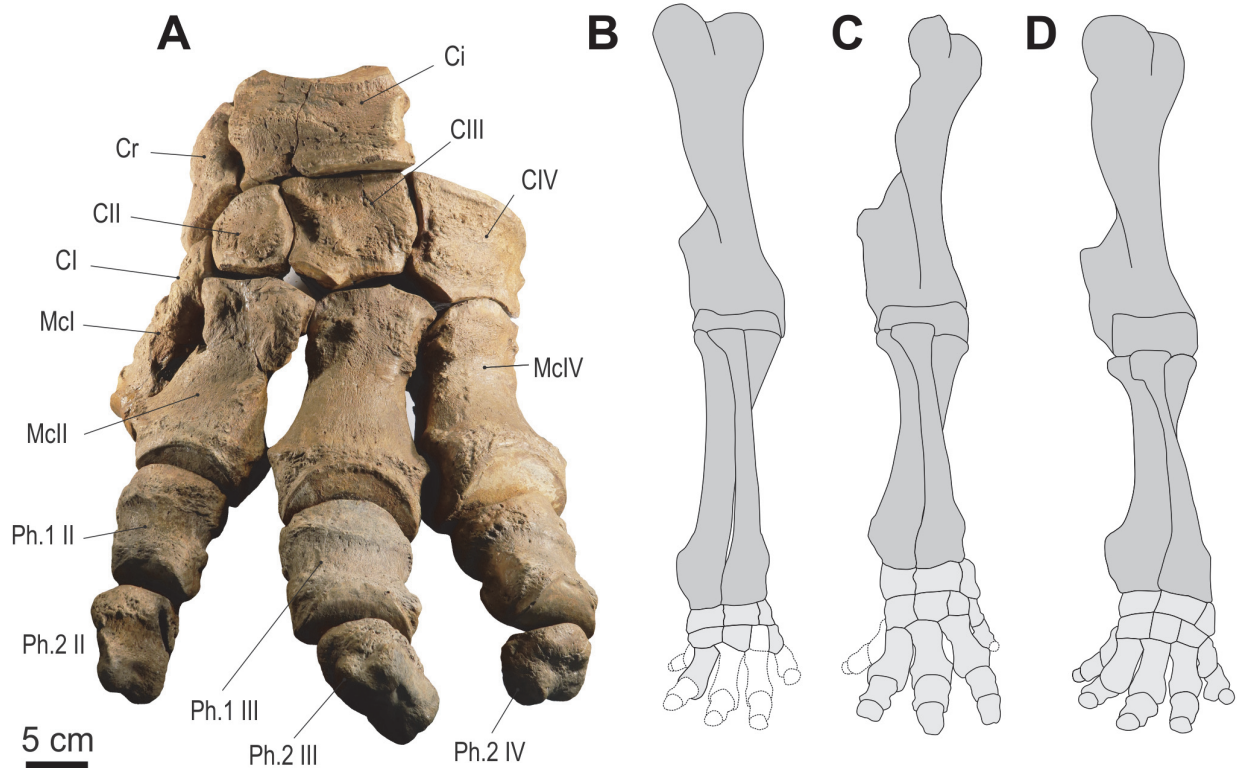
FIGURE 9. Left manus of *"Mammut" borsoni* from Kaltensundheim. **A:** Dorsal aspect of the left articulated hand skeleton. **B-D:** Comparison of proportions in mammutid forelimbs. **B:** *Z. turicensis* group (Turgai KAS, Mikulov-Czujan's sandpit CZ); **C:** *"Mammut" borsoni* (individual from Kaltensundheim DE); and **D:** *Mammut americanum* (individual from Fort Wayne-Bueshing, from UMORF). **Abbreviations:** Cr – radiale, Ci – intermedium, CI-CIV – carpalia I-IV; McI-McIV – metacarpalia I-IV; Ph 1-Ph 2 – proximal and medial phalanges of digits I-IV.

The Cu of *"M". borsoni* from Kaltensundheim and those of *M. americanum* are proximodistally lower than in *Z. turicensis*; but the palmar articular facet for the Ca in both taxa is higher than in *Z. turicensis* and forms a more prominent edge with the proximal facet for the ulna. The lateral part of the proximal ulna facet is more concave in *"M". borsoni* from Kaltensundheim and *M. americanum* than in *Z. turicensis*.

The left accessorium (Ca, pisiforme) (23) (Figure 11S-X, Table 4) is proximodistally elongated and irregularly "dumbbell" shaped. The proximal facet for the ulna is slightly concave and semicircular and contacts in a straight line the proximodorsally facing facet for the Cu, which is flat and rounded triangular in outline. The shaft ends in a distal rugose protuberance. The palmar side of the shaft is convex and rugose, while there is a smooth, twisting sulcus along the dorsal side from proximal mediovolar to distodorsal.

The Ca of *"M". borsoni* from Kaltensundheim is dorsopalmarly somewhat flatter and in its midshaft more constricted than in *M. americanum*.

There is no Ca of *Z. turicensis* available for comparison.

All elements of the distal row of carpalia (Figures 5, 12) of the left hand are preserved: carpale primum (CI = trapezium), carpale secundum (CII = trapezoideum), the carpale tertium (CIII = magnum), and carpale quatrum (CIV = hamatum, unciforme). Their proximal and distal articulation counterparts are indicated in Figure 10.

The articulation between CIII and CIV from the distal row and Cu and Ci from the proximal row is in serial arrangement, whereas the articulation of CII and CIII of the distal row and the Ci and Cr of the proximal row are in aserial arrangement. The carpals of the distal row articulate distally with the metacarpals I-V (Figure 9).

The left carpale I (33) (carpale primum, trapezium) (Figure 12B-F, Table 5) is mediolaterally flattened and approximately trapezoid in medial view, tapering palmarly. The proximal facet for the Cr is semicircular with a straight lateral border, flat, and facing proximopalmarly. The adjacent lateral facet for CII is irregular in shape, tapering palmarly, and
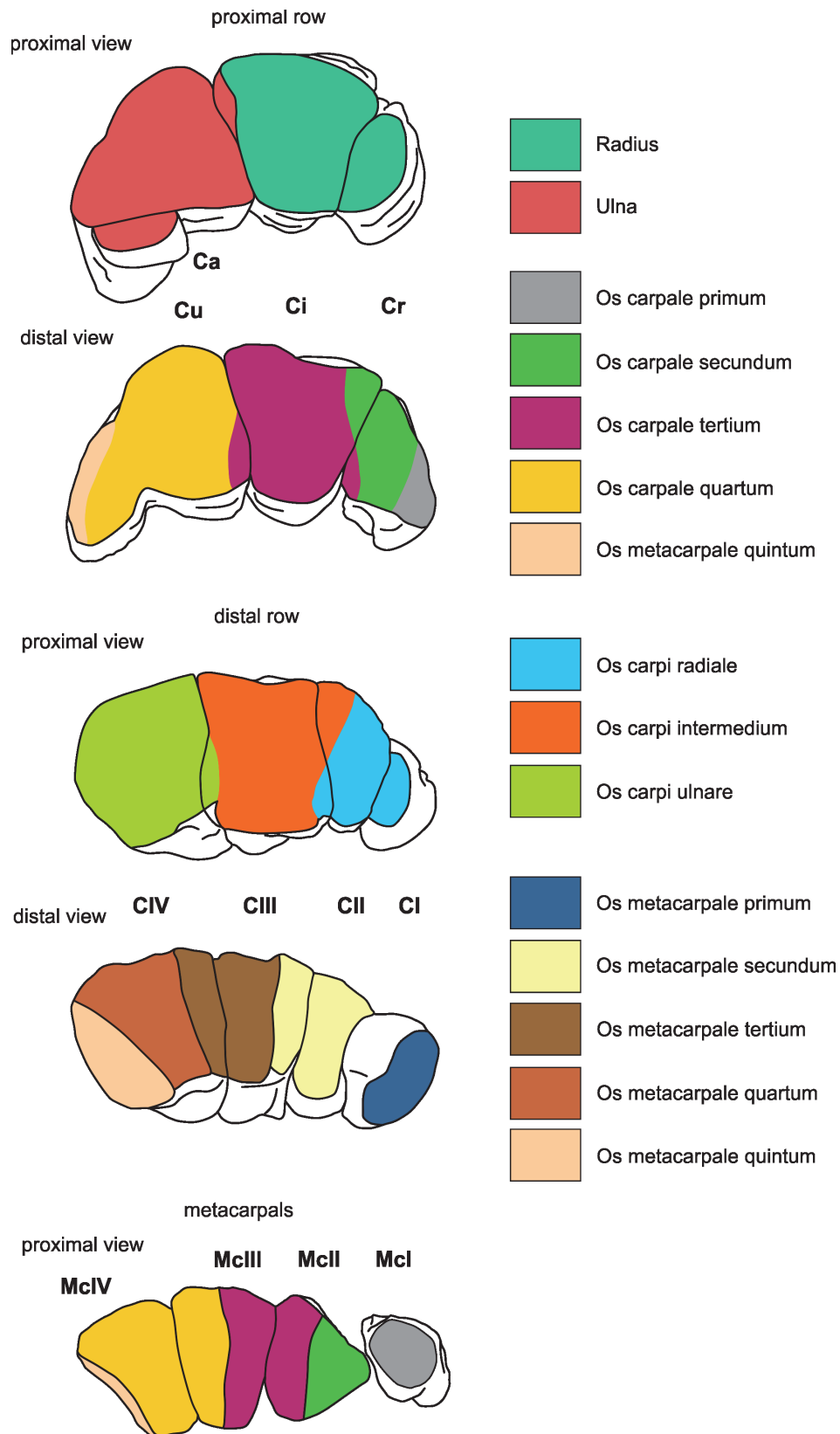
FIGURE 10. Articulation of carpus of *"Mammut" borsoni* from Kaltensundheim. The colors indicate to which bone each specific facet of the carpals and metacarpals articulates.
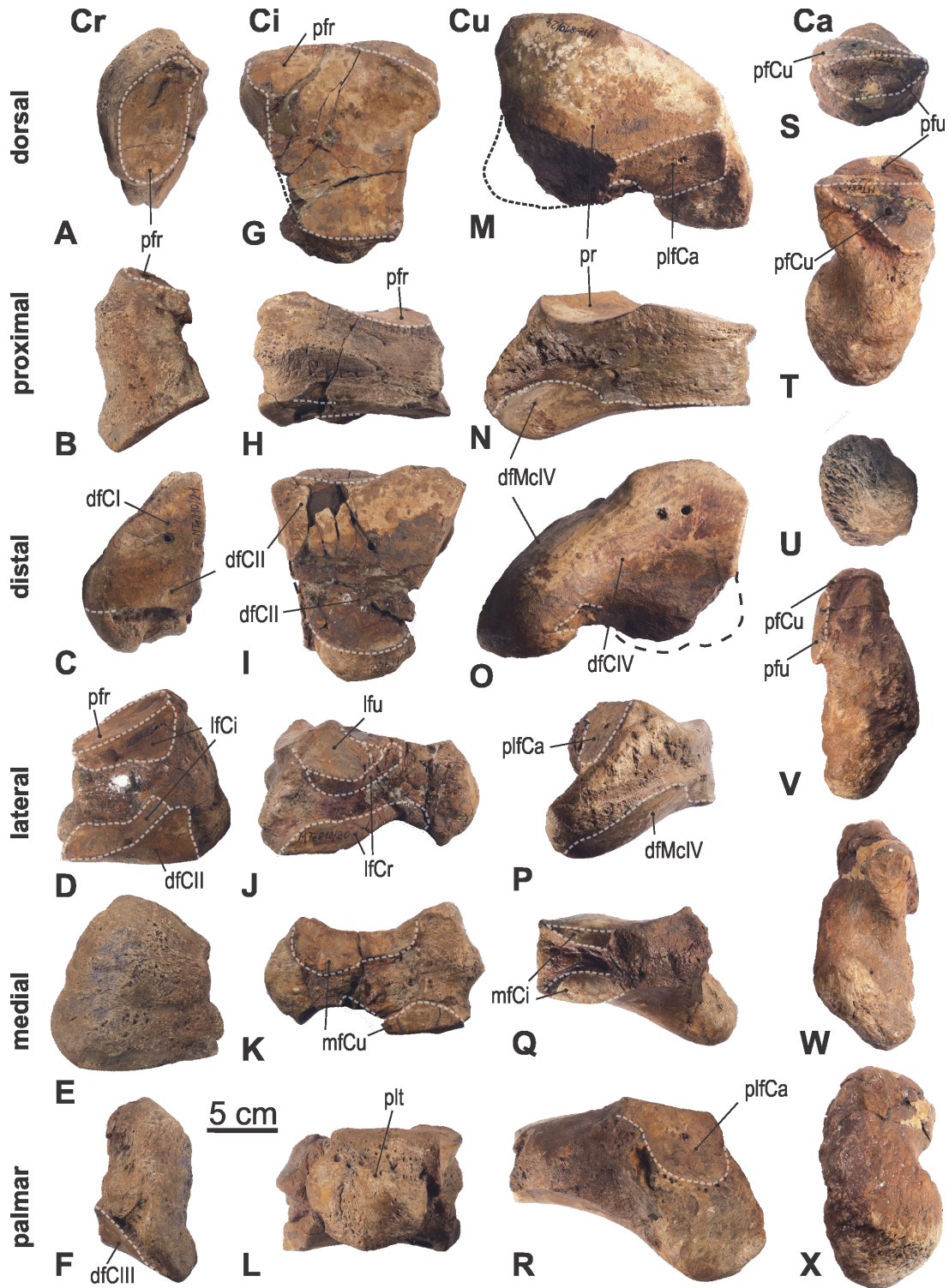
FIGURE 11. Proximal row of carpalia of *"Mammut" borsoni* from Kaltensundheim. **A-F:** Cr = Os carpi radiale sin (scaphoideum) (NHMS-MTe 810/21), **G-L:** Ci = Os carpi intermedium sin (lunatum) (NHMS-MTe 810/20), **M-R:** Cu = Os carpi ulnare dext (cuneiforme) (mirrored) (NHMS-MTe 810/24), **S-X:** Ca = Os carpi accessorium sin (pisiforme) (NHM-MTe 810/23). **Abbreviations:** dfCI – distal facet for CI, dfCII – distal facet for CII, dfCIII – distal facet forCIII, dfCIV – distal facet for CIV, dfMcIV – distal facet for McIV, lfCi – lateral facet for Ci, lfCr – lateral facet for Cr, lfu – lateral facet for ulna, mfCa – medial facet for Ca, mfCi – medial facet for Ci, pfCu – proximal facet for Cu, plfCa – palmar facet for Ca, pfr – proximal facet for radius, pfu – proximal facet for ulna, plt – palmar tuberosity.
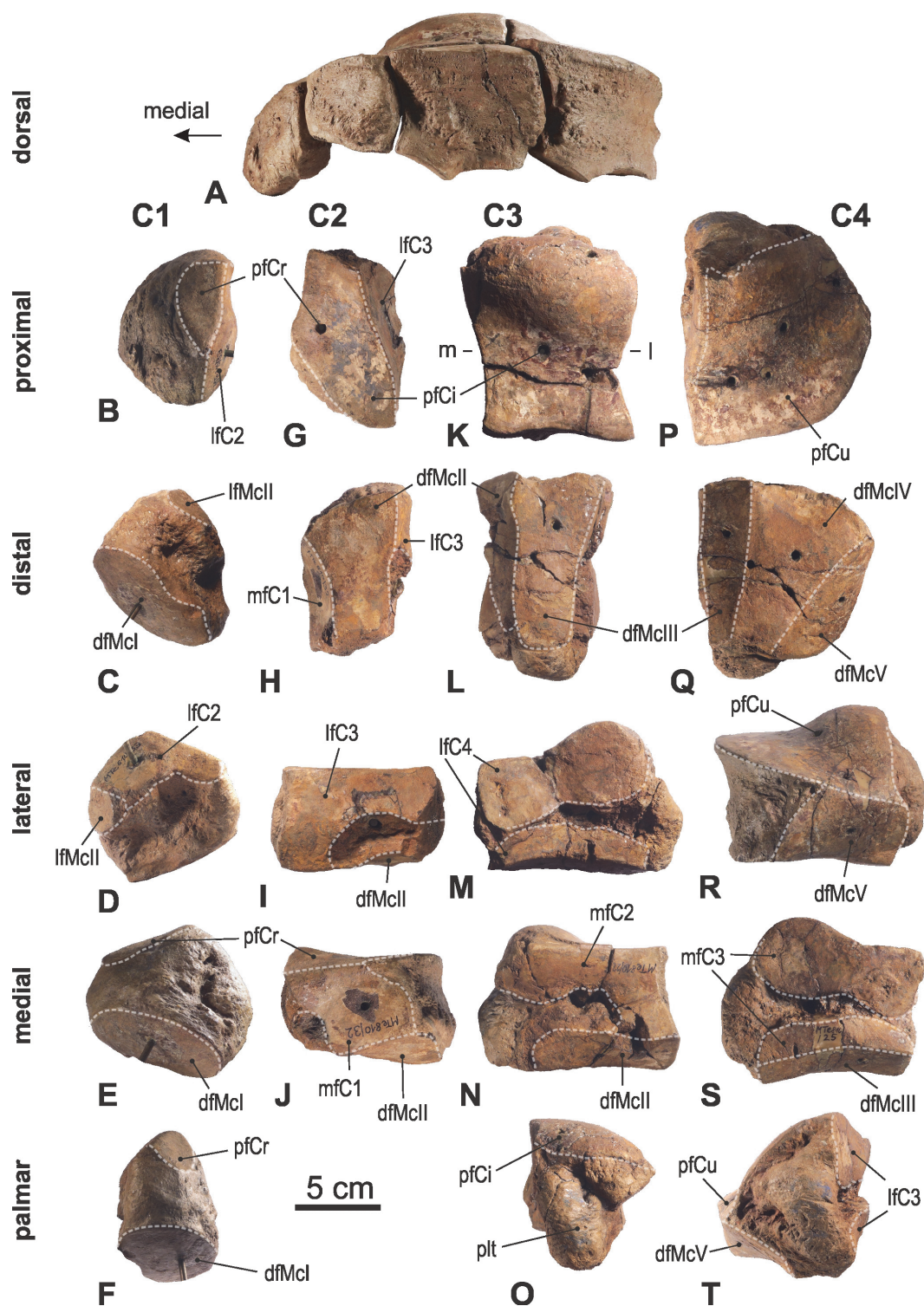
FIGURE 12. Distal row of left carpalia of *"Mammut" borsoni* from Kaltensundheim. **A:** distal row of left carpalia in articulation in dorsal view, **B-F:** CI = trapezium (NHMS-MTe 810/33), **G-J:** CII = trapezoideum (NHMS-MTe 810/32), **K-O:** CIII = magnum (NHMS-MTe 810/22), **P-T:** CIV = hamatum (NHMS-MTte 810/25). **Abbreviations:** dfMcI – distal facet for McI, dfMcII – distal facet for McII, dfMcIII – distal facet for McIII, dfMcIV – distal facet for McIV, dfMcV – distal facet for McV, lfCII – lateral facet for CII, lfCIII – lateral facet for CIII, lfCIV –lateral facet for CIV, lfMcII – lateral facet for McII, mfCI – medial facet for CI, mfCII – medial facet for CII, mfCIII – medial facet for CIII, pfCII – proximal facet for CII, pfCr – proximal facet for Cr, pfCu – proximal facet for Cu, pfCi – proximal facet for Ci, pfMcI – proximal facet for McI, plt – palmar tuberosity.

FIGURE 13. Left metacarpal bones of *"Mammut" borsoni* from Kaltensundheim: **A-E:** McIV (NHMS-MTe 810/28), **F-J:** McIII (NHMS-MTe 810/29), **K-O:** McII (NHMS-MTe 810/35), **P-T:** McI (NHMS-MTe 810/34). **Abbreviations:** lfMcIII – lateral facet for McIII, lfMcIV – lateral facet for McIV, lfMcV – lateral facet for McV, mfMcII – medial facet for McII, mfM-cIII – medial facet for McIII, mfMcI – medial facet for McI, pfCI – proximal facet for CI, pfCII – proximal facet for CII, pfCIII – proximal facet for CIII, pfCIV – proximal facet for CIV, tMc – trochlea metacarpalis.
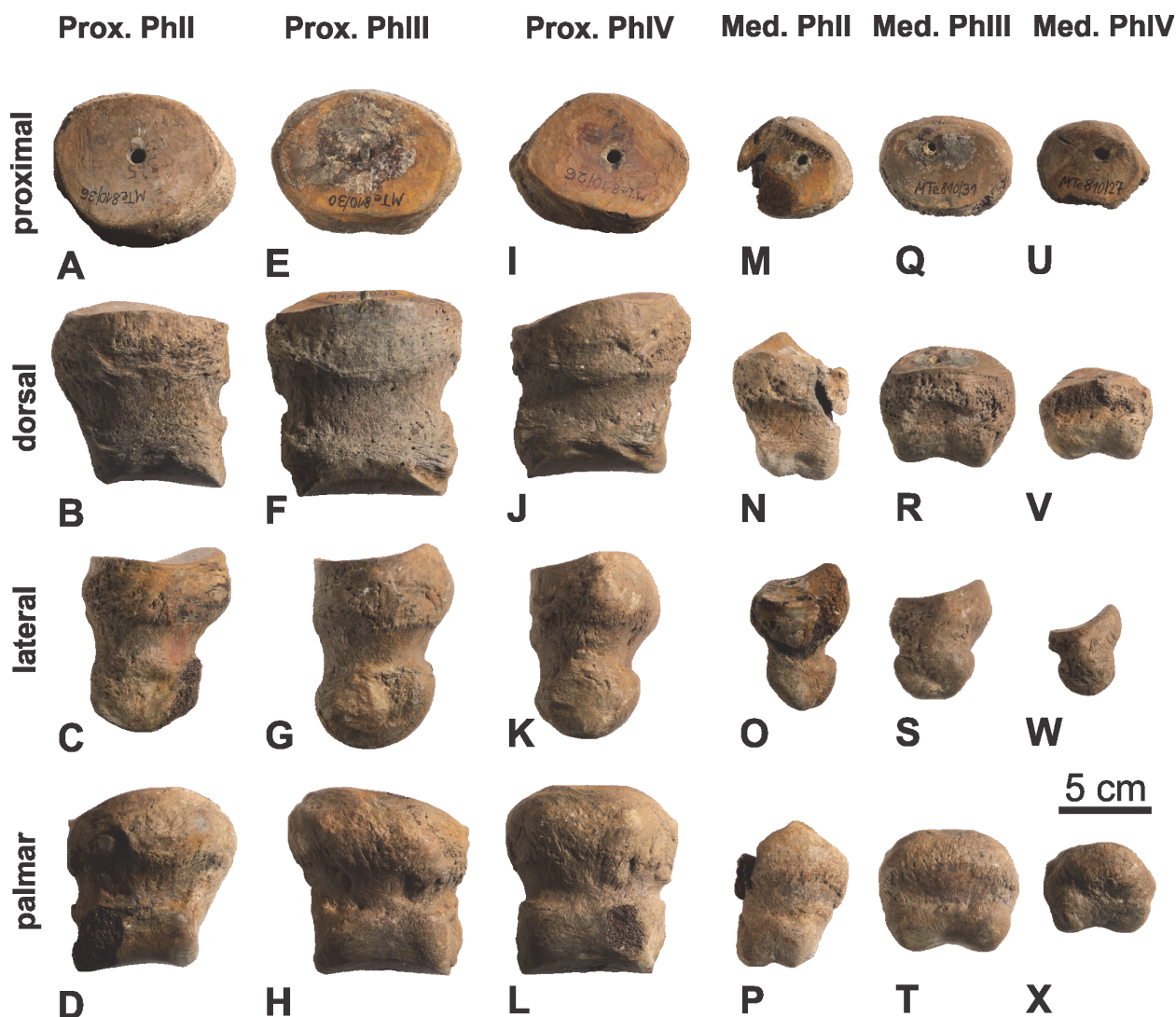
FIGURE 14. Proximal and medial phalages of the left hand of *"Mammut" borsoni* from Kaltensundheim. **A-D:** phalanx proximalis II (NHMS-MTe 810/36), **E-H:** phalanx proximalis III (NHMS-MTe 810/30), **I-L:** phalanx proximalis IV (NHMS-MTe 810/26), **M-P:** phalanx medialis II (NHMS-MTe 810/37), **Q-T:** phalanx medialis III (NHMS-MTe 810/21), **U-X:** phalanx medialis IV (NHMS-MTe 810/27).

slightly convex. This lateral CII-facet and the proximal Cr-facet contact each other along a straight edge. There is a small rounded facet for the McII, which faces laterodorsodistally. The lateral CII-facet also contacts this McII-facet along an edge. The medial and palmar sides of the CI are convex, whereas the lateral surface shows an irregular depression. The distal facet for the McI is oval and large, covering the entire distal end and is slightly convex. It is facing distomedially.

The CI of *"M". borsoni* from Kaltensundheim is mediolaterally more flattened and less massive than in *M. americanum.* The facet for the CII is somewhat smaller and less square than in *M. americanum.* The distal facet for the McI is oval

elipsoid in Kaltensundheim whereas rounded triangular in *M. americanum*. There is no CI of *Z. turicensis* available for comparison.

The left carpale II (32) (carpale secundum, trapezoideum) (Figure 12G-J, Table 5) (missing its palmar end) is a narrow and low bone. In proximal view, its overall shape is irregular trapezoid tapering palmarly, while the dorsopalmar depth increases laterally. The proximal facet is triangular and slightly saddle-shaped – dorsopalmarly concave and mediolaterally convex; it articulates primarily with the Cr and in its dorsolateral segment with the Ci. The distal facet for the McII is trapezoid, narrowing palmarly and slightly concave. The medial facet for the CI is slightly concave in dor-
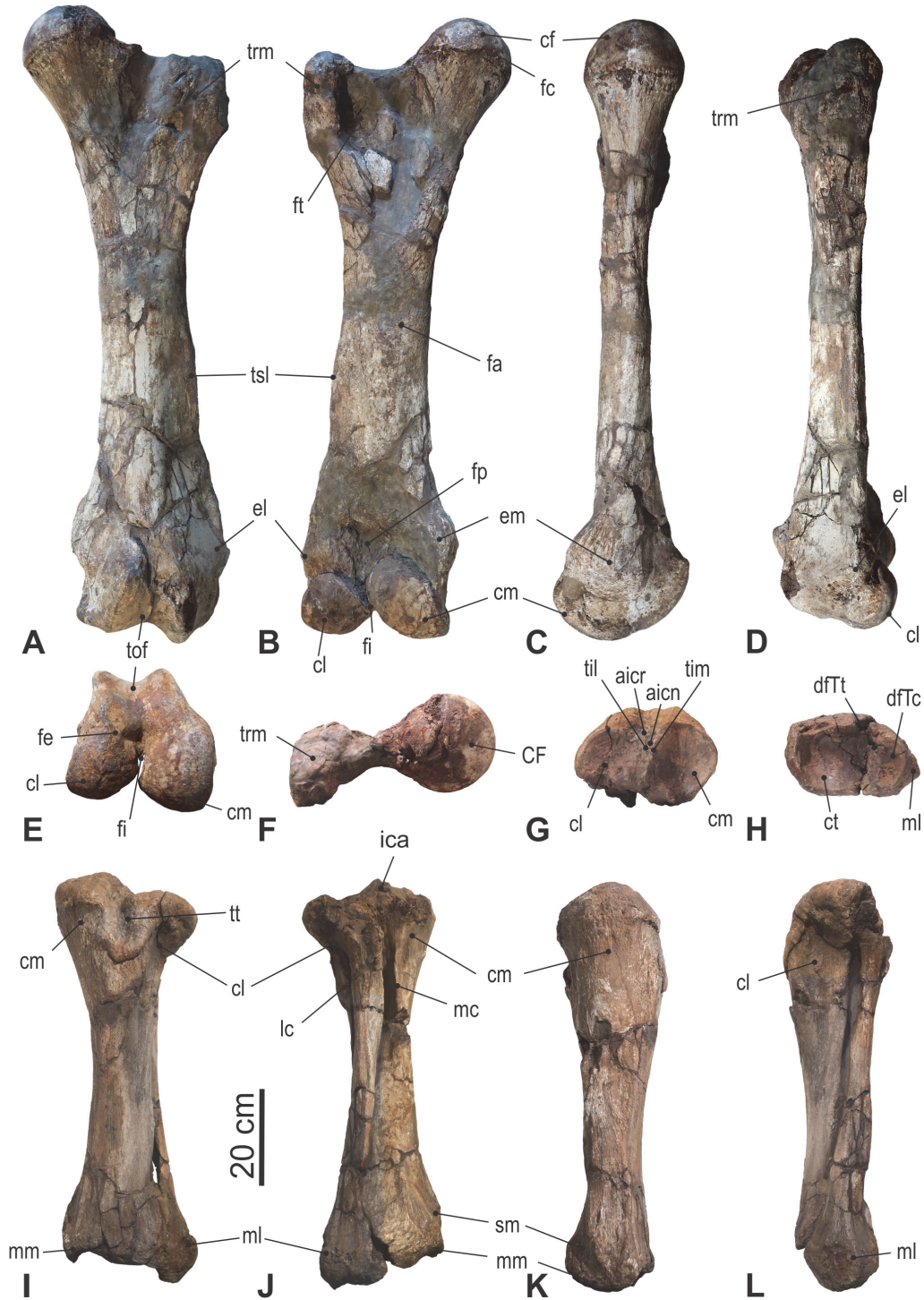
25

FIGURE 15. Long bones of the hindlimb of *"Mammut" borsoni* from Kaltensundheim. **A-F:** femur sin (NHMS-MTe 810/8), **G-L:** Tibia and fibula sin in articulation (NHMS-MTe 810/5). **Views:** A – cranial, B – caudal, C and K – medial, D and L – lateral, E and H – distal, F and G – proximal, I – dorsal, J – plantar. **Abbreviations:** aicn – area intercondylare centralis, aicr – area intercondylare cranialis, cf – caput femoris, cl – condylus lateralis, cm – condylus medialis, ct - cochlea tibiae, dfTc – distal facet for Tc, dfTt – distal facet forTt, el – epicondylus lateralis, em – epicondylus medialis, fa – facies aspera, fc – fovea capitis, fe – fossa extensoria, fi – fossa intercondylaris, fp – facies poplitea, ft – fossa trochanterica, mc – medial crest, ml – malleolus lateralis, mm – malleolus medialis, sm – sulcus malleolaris, til – tuberculum intercondylare lateralis, tim – tuberculum intercondylare medialis, tof – trochlea ossis femoris, trmj – trochanter major, tsll – tuberositas supracondylaris lateralis, tt – tuberositas tibiae.
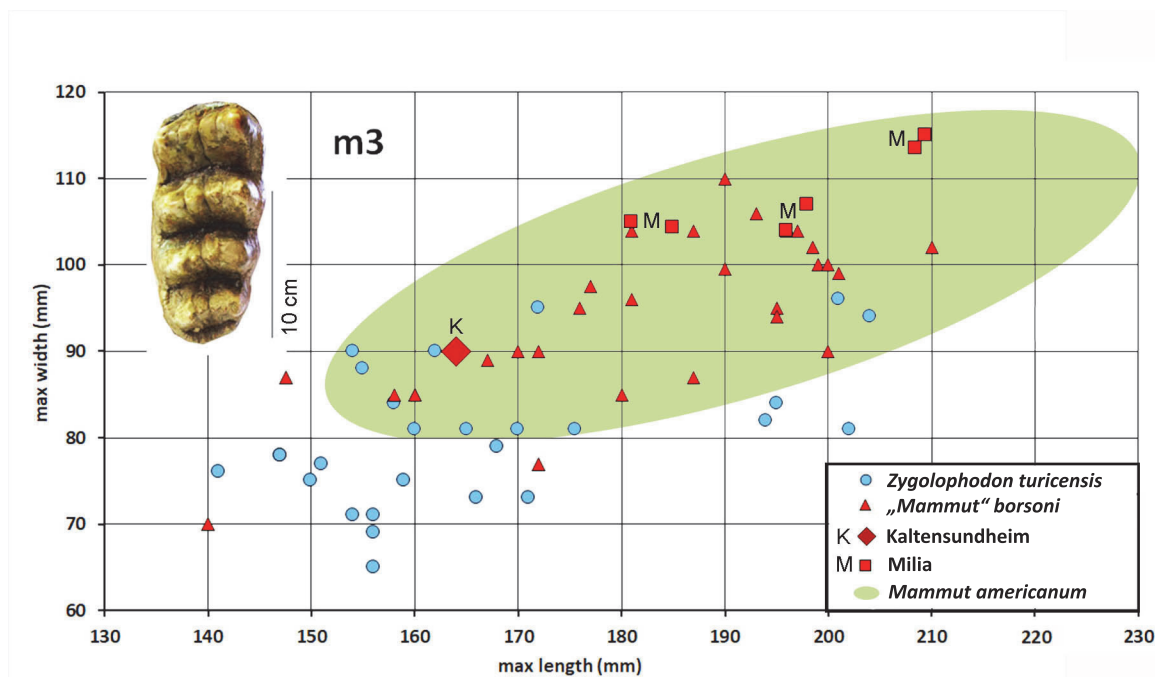
FIGURE 16. Metrical variability of the m3 in *Zygolophodon turicensis* (blue) and *"Mammut" borsoni* (red, Table 7), compared to the approximate variability of the m3 in *Mammut americanum* (green) (data for *M. americanum* from Dooley et al., 2019, figure 32). The m3 from Kaltensundheim (K) is relatively small compared to other specimens from Central Europe, especially Milia (M).

sopalmar direction and covers almost the entire medial surface except its distodorsal corner. The lateral facet for the CIII is L-shaped with its maximal height dorsally and slightly convex.

The CII of *"M". borsoni* from Kaltensundheim tapers (in proximal view) in palmar direction, but in *M. americanum* the bone narrows quite abruptly forming a distinct waist (especially on the lateral side), so that the palmar portion of the CII is distinctly narrower than the dorsal part. As a consequence, the lateral facet for the CIII is strongly curved. It seems, that in *M. americanum* the CII can be occasionally bipartite - split in two small bones, a dorsal and a smaller palmar one, articulating with each other. Such condition is developed, e.g., in the right hand (but not in the left one!) of the Buesching mastodon and in the Hyde Park mastodon (Fisher, 2008). But it is difficult to investigate the development or variability of the CII within mammutids in more detail, because it is rarely documented. No CII (trapezoid) is known of *"M". borsoni* from Milia (Greece), but one is described from the Villafranchian of Velenje (Slovenia) (Rakovec, 1997), which is not bipartite. No CII is known of *Z. turicensis*. So far, occasional bipartite CII are known only of *M. americanum*.

The left carpale III (22) (carpale tertium, magnum) (Figure 12K-O, Table 5) is a massive bone, increasing in height in palmar direction and almost square in proximal and dorsal aspect. The proximal facet is nearly rectangular in shape, with slightly concave medial, lateral, and dorsal borders; its palmar half is domed convex while its dorsal half is almost flat. The proximal facet articulates largely with the Ci, only in its palmomedial and palmolateral corners it articulates with the Cr and the Cu, respectively. The distal facet for the McIII is narrow, trapezoid, tapering palmarly, and slightly concave in dorsopalmar direction. The distal facet for the McII faces mediodistally, is mediolaterally narrow, and almost flat. The distal facets for McII and III form an angle of about 140°. The medial facet for the CII is L-shaped with its dorsal part being the highest and contacting the distal facet for the McII along an edge. On the lateral side, there are two facets for the CIV, which almost contact each other dorsally, but diverge palmarly; the large proximal one is waisted and slightly concavely flexed in the middle, the distal one is elongated, low and slightly concave in its middle.

In proximal aspect, the CIII of *"M". borsoni* from Kaltensundheim is almost rectangular in outline, whereas in *M. americanum*, in *Z. turicensis*

TABLE 7. Comparative measurements of lower m3 of *"Mammut" borsoni* from Kaltensundheim with values of *"Mammut" borsoni* and of *Zygolophodon turicensis* from selected European localities.

Locality	Taxon	max length	max width	L/W	Wx100/L	Source
Strekov (SK), MN17	*"M." borsoni*	160*	85	1.89	53	SNM; Holec, 1985
Strekov (SK), MN17	*"M." borsoni*	147.6	87.1	1.69	59	Schmidt-Holouzka, 1970
Strekov (SK), MN17	*"M." borsoni*	215	102.2	2.06	48	Holec, 1985
Nova Vieska (SK) MN17	*"M." borsoni*	201	99	2.03	49	SNM,
Kaltensundheim (DE), MN16-17	*"M." borsoni*	164	90	2.73	36	own measurements
Sülzfeld (DE)	*"M." borsoni*	172	103	1.66	60	own measurements
Sülzfeld (DE)	*"M." borsoni*	187	104	1.80	55	own measurements
Hajnáčka (SK), MN 16a	*"M." borsoni*	196	104	1.88	53	Fejfar, 1964
Hajnáčka (SK), MN16a	*"M." borsoni*	195	94	2.07	48	Schlesinger, 1922
Vialette (FR), MN16	*"M." borsoni*	181	104	1.74	57	own measurements, and Lortet and Chantre, 1878
Vialette (FR), MN16	*"M." borsoni*	195	95	1.87	53	Lortet and Chantre, 1878
Milia (GR), MN15	*"M." borsoni*	185	104.3	1.77	56	Tsoukala and Mol, 2016
Milia (GR), MN15	*"M." borsoni*	181	105	1.72	58	Tsoukala and Mol, 2016
Milia (GR), MN15	*"M." borsoni*	208.4	113.5	1.84	54	Tsoukala and Mol, 2016
Milia (GR), MN15	*"M." borsoni*	209.4	115	1.82	55	Tsoukala and Mol, 2016
Milia (GR), MN15	*"M." borsoni*	196	104	1.88	53	Tsoukala and Mol, 2016
Milia (GR), MN15	*"M." borsoni*	198	107	1.85	54	Tsoukala and Mol, 2016
Audrey. (Haute-Saone) (FR), Pliocene	*"M." borsoni*	177	97	1.82	55	own measurements
Buisson-la-Ville near Audrey (FR), Pliocene	*"M." borsoni*	190	99.5	1.90	52	own measurements
Gros Roland near Issoire (FR), Pliocene	*"M." borsoni*	181	96	1.88	53	own measurements
Grimolais (FR), Pliocene	*"M." borsoni*	193	106	1.82	55	own measurements, and Lortet and Chantre, 1878
Wörth am Rhein (DE), Pliozän	*"M." borsoni*	158	85	1.85	54	Maße R. Ziegler (SMNS)
Alt-Lichtenwarth (AT), MN14-16	*"M." borsoni*	198.5	102	1.95	51	Thenius, 1987
Ahmatovo (BUL), Levantin	*"M." obliquelophus*	176	95	1.85	54	Nikolov and Kovačev, 1966
Ahmatovo (BUL), Levantin	*"M." obliquelophus*	167	89	1.88	53	Nikolov and Kovačev, 1966
	Z. turicensis	159	75	2.12	47	Göhlich, 1998
Wolkersdorf (Rochusberg) (AT), MN9-11	*Z. turicensis*	160	81	1.80	56	own measurements

from Mikulov-Czujan's sandpit (Březina, 2014) and in *"M". borsoni* from Velenje (Rakovec, 1997) the bone forms a strong mediopalmar projection, so that the medial side is strongly curved. Such a strong medial step joint prevents any dorsopalmar gliding movements between CII and CIII. However, the absence of such a mediopalmar extension on the CIII from Kaltensundheim seems to be intraspecific variability, as it is present in *"M". borsoni* from Velenje. On the lateral side, the proximal facet for the CIV is slightly flexed concave in *"M". borsoni* from Kaltensundheim and Velenje, but flat in *M.*

americanum and *Z. turicensis*. A distal facet for McII is present in *"M". borsoni* from Kaltensundheim and Velenje and in *M. americanum*, but missing in *Z. turicensis* (Mikulov-Czujan's sandpit). In *"M". borsoni* from Kaltensundheim and in *M. americanum* the entire bone narrows distally, carrying two facets – for the McII and III – whereas the CIII of *Z. turicensis* does not narrow distally and provides only a single, but larger distal facet for the McIII (a facet for McII is not developed). A CIII of *"M". borsoni* from Milia (Greece) was neither described nor figured.

TABLE 7 (continued).

Locality	Taxon	max length	max width	L/W	Wx100/L	Source
Mikulov (Czujan's pit), MN7/8	*Z. turicensis*	154	71	2.17	46	own measurements
Mikulov (Czujan's pit), MN7/8	*Z. turicensis*	147	78	1.88	53	own measurements
Mikulov (Czujan's pit), MN7/8	*Z. turicensis*	(150)	(75)	2	5	own measurements
Mikulov (Czujan's pit), MN7/8	*Z. turicensis*	168	79	2.13	47	own measurements
Mikulov (Czujan's pit), MN7/8	*Z. turicensis*	171	73	2.34	42	own measurements
Mikulov (Czujan's pit,) MN7/8	*Z. turicensis*	166	73	22.27	44	own measurements
Freising (DE), MN6-7/8	*Z. turicensis*	147	87	1.69	59	Lehmann, 1950
Freising (DE), MN6-7/8	*Z. turicensis*	141	76	1.85	54	Lehmann, 1950
Tutzing (DE), MN6-7/8	*Z. turicensis*	155	88	1.76	57	Lehmann, 1950
Tutzing (DE), MN6-7/8	*Z. turicensis*	155	88	1.76	57	Lehmann, 1950
Simorre (FR), MN6-MN7/8	*Z. turicensis*	156	69	2.26	44	Tassy, 1977
Malartic (FR), MN6	*Z. turicensis*	202	81	2.49	40	Tassy, 1977
Malartic (FR,) MN6	*Z. turicensis*	151	69	2.19	46	Tassy, 1977
Malartic (FR,) MN6	*Z. turicensis*	158	64	2.47	40	Tassy, 1977
Malartic (FR), MN6	*Z. turicensis*	204	94	2.17	46	Tassy, 1977
Malartic (FR), MN6	*Z. turicensis*	201	96	2.09	48	Tassy, 1977
Malartic (FR), MN6	*Z. turicensis*	159	75	2.12	47	Tassy, 1977
Kalksburg (AT), MN5-6	*Z. turicensis*	165	81	2.04	49	Schlesinger, 1917
Poysdorf (AT), MN5-6	*Z. turicensis*	211	87	2.42	41	Schlesinger, 1917
Klein-Hadersdorf (AT), ?MN5-6	*Z. turicensis*	156	65	2.40	42	Schlesinger, 1917
Rajégats (FR), MN6	*Z. turicensis*	204	94	2.17	46	Tassy, 1985
Rajégats (FR), MN6	*Z. turicensis*	201	96	2.13	47	Tassy, 1985
Hidvég (SK)	*Z. turicensis*	199	100	1.99	50	Holec, 1985
Szabadka (SK)	*Z. turicensis*	160	85	1.88	53	Holec, 1985
Vácz (SK)	*Z. turicensis*	200	90	2.22	45	Holec, 1985
Turgai (KAS) Early Miocene	*Z. atavus*	163	90	1.81	55	Borissiak, 1936
Turgai (KAS) Early Miocene	*Z. atavus*	172	95	1.81	55	Borissiak, 1936

The left carpale IV (25) (carpale quartum, hamatum, unciforme) (Figure 12P-T, Table 5) is a massive bone and in overall shape wedge like, with a flat and high medial side and lowering laterally. In proximal aspect, the outline is nearly semicircular. A big proximal facet, which exclusively articulates with the Cu, is convex lateromedially and domes towards the palmomedial corner, where the bone is the highest. The distal side is covered by three facets side by side, but angled to each other. The distal facet for the McIV is trapezoid, tapering palmarly, and slightly concave in dorsopalmar direction. The distal facet for the McIII is narrower, almost square, faces mediodistally, and is slightly concave dorsopalmarly. The distal facet for the McV is rhombic, flat, and faces distolaterally; its dorsal border contacts the proximal facet for the

Cu. The distal facets for McII and III form an angle of about 140°. The medial side carries two facets for the CIV, which almost contact each other dorsally, but diverge palmarly; the large proximal one is slightly constricted and slightly convex dorsopalmarly in the middle; the distal one is longitudinal, low, and weakly convex in its middle.

The CIV of *"M". borsoni* from Kaltensundheim and Velenje and of *M. americanum* are very similar in morphology. Only the distance between the two medial facets for the CIII is somewhat narrower in the Kaltensundheim specimen, than in *"M". borsoni* from Velenje and in *M. americanum*. Thus, this difference is not diagnostic. No CIV is available for comparison of *Z. turicensis* from Mikulov and of *"M". borsoni* from Milia not described.

TABLE 8. Mandible measurements (mm) of Mammutidae and comparison of the symphysis length in relation to the length of m2+m3.

locality	taxon	length of symphysis	length m2+m3	mandibular tusk	ratio symph/ m2+m3	source
Fort Wayne, USA (Buesching Mastodon)	*M. americanum*	140	235	lacking	0.59	UMORF
Hyde Park, USA	*M. americanum*	135	273	lacking	0,49	Fisher 2008
D'Autrey, FR	*"M." borsoni*	110	270	present	0,41	Bergouniou and Crouzel 1961, own measurements
Kaltensundheim, DE	*"M." borsoni*	~245	266	present	0.92	this study
Milia, GR	*"M." borsoni,* MIL 143	310 ventral 280 dorsal	310	present	1.00 0.9	Tsoukala 2000, tab. 1
Milia, GR	*"M." borsoni,* MIL 562/563	ca. 190	325	alveolus present	0,58	Tsoukala and Mol 2016, table 4
Vialette (juv.), FR	*"M." borsoni*	very brevirostrine	(m1+2)	lacking	0.68	Lortet and Chantre 1878
Farladani, MOL	*"M." borsoni*	--	--	present	0.97	Pavlow 1893, ratio measured from plate 3, figure 5
Nikolajew, UA	*"M." borsoni*	very brevirostrine	ca. 330	present	ca.0.4	Brandt 1860 (measured from plate 1), Pavlow 1894
Shanxi (Shansi), CHN	*"M." borsoni* (= *Z. shansiensis*), juv.	symphysis restored	m1-m3 415		0.54	Hopwood 1935, plate 6, figure 5, ratio measured from Tobien 1988, figure 63b
Belka, UA	*"T." turicensis* (=obliquelophus or *"M." borsoni*)	very juvenile	--	present	0,69	Korotkevich 1988, figure 25
Ahmatovo, BUL	*"M." obliquelophus*	350	ca. 271	alveolus present	1.3	Nikolov and Kovačev1966, Markov 2008
Romanovka, UA	*"M." obliquelophus*	296	sin/dext 294/287	present	1.01-1.03	Mucha 1980
Balta?, Podolia, UA	*"M." praetypicum*	305	292	present	1.04	Kubiak 1972
Petchana, Podolia, UA	*"M." ohioticus* (= *borsoni*)	short	--	lacking, no alveolus	--	Pavlow 1894
Freising, DE	*Z. turicensis*	symphysis restored	--	present	0.83	Lehmann, 1950, ratio measured from plate 14, figure 26
Wolkersdorf, AT	*Z. turicensis*	ca. 120	266	lacking	0.45	own measurements
Villefranched'Astarac, FR	*Z. turicensis*	ca. 410, but symphysis largely restored	250	present	1.64	Pontier 1926, measured from plate 8. Duranthon et al. 1995
Turgai, KAS	*Z. "atavus"*	--	sin/dext 292/281	present	1.51	Borissiak 1936, ratio measured, from plate 1, figure 4
Tung Gur, CHN	*Z. gobiensis*	420	320	present	1.31	Tobien et al. 1988, measured from figure 39

Metacarpalia (Figure 13, Table 6)

The metacarpals I-IV of the left hand are preserved, McV is not available. The epiphyses of all metacarpals are all fully fused, without any visible suture. McIII is the longest of the metacarpals. McI is the shortest and about 60% of the length of McIII.

The left metacarpale I (34) (Figure 13P-T, Table 6) is missing the lateral margin of the trochlea. The proximal end is palmarly extended forming a protuberance. The proximal facet for the CI is

oval, flat, and slightly laterally inclined. As is typical for a marginal digit, the distal trochlea is somewhat asymmetrical, with the axis of the trochlea being slightly deflected. The dorsal part of the trochlea is low.

The left metacarpale II (35) (Figure 13K-O, Table 6) is missing its proximopalmar part and some pieces of the midshaft where the bone was broken. The overall shape of the McII (in dorsal/ palmar aspect) appears distorted as the proximal half of the bone is shifted laterally and is therefore more asymmetric than McIII and IV. The proximal facet for the CII is triangular, slightly concave and faces slightly proximomedially. The adjacent proximal facet for the CIII is rectangular, flat and separated from the CII-facet by a curved edge, which is more distinct in its palmar half. Situated on the medial side of the proximal end is a small, flat, and semicircular facet for articulation with the CI. On the lateral side of the proximal end runs an extended semicircular facet for McIII. There is a swollen protuberance dorsolaterally on the proximal end. The cross-section of the mid-shaft is rounded-triangular. The distal trochlea reaches higher (in proximal direction) on the palmar side than on the dorsal side. On the palmar side the proximal extension of the trochlea is strongly asymmetric and distinctly declines in height towards medially. There is a strong protuberance for a ligament on the medial side of the distal end.

The proximal end of the McII of *"M". borsoni* from Kaltensundheim is relatively broader, lateromedially than in *Z. turicensis* and *M. americanum*. It also is distinguished from the latter two in having a larger medial CII-facet. The proximal end of *M. americanum* (Buesching specimen) differs from the Kaltensundheim specimen and *Z. turicensis* by having a strongly concave medial incision on the articular facet for CII. The edge between the proximal facets for CII and CIII is curved in *"M". borsoni* from Kaltensundheim and in *M. americanum*, but straight in *Z. turicensis*. Furthermore, both taxa differ from *Z. turicensis* by a proximodistally higher lateral McIII-facet.

The left metacarpale III (29) (Figure 13F-J, Table 6) is complete and the largest of the Mc-series. In dorsal aspect, the proximal end only extends on its lateral side. Both proximal facets, for articulation with CII and CIII, are of similar size, almost rectangular, and clearly separated by a slightly curved edge forming at the highest point of the bone. The CIII-facet is slightly concave, whereas the CIV-facet is almost flat and facing slightly proximomedially. On both sides of the prox-

imal end, there is an adjacent medial and lateral facet for the McII and McIII, respectively; they are dorsodistally extended and flat. The medial McII-facet is incomplete palmarly. The shaft is dorsopalmarly flattened and slightly pyriform in cross-section. A distinct longitudinal (proximodistally) crest runs along the palmomedial half of the shaft. On the medial and lateral side of the distal end are strong protuberances for ligament attachments. They form the largest width of the bone. The distal trochlea is higher palmarly than dorsally. On the palmar side, the trochlea is damaged in its medial half. The palmar part of the trochlea is devided by a distinct sagittal bulge in two equally sized facets for the sesamoids.

The McIII of *"M". borsoni* from Kaltensundheim and from Velenje (Rakovec, 1997) are morphologically very similar. Whereas the proximal facets for CII and CIII are almost equal in size in the Kaltensundheim specimen, the CIII-facet seems slightly larger in *"M". borsoni* from Velenje and in *M. americanum*, but which is obviously not of any taxonomic importance. No McIII of *Z. turicensis* is known.

The left metacarpale IV (28) (Figure 13A-E, Table 6) is complete, slightly shorter than McIII, but longer than the McII; at its distal shaft it is the mediolaterally widest of all preserved metacarpals. In dorsal aspect, the proximal end is laterally flexed, as the lateral side is broadened while the medial side is laterally inclined. The proximal facet for articulation with the CIV is rounded-triangular and slightly saddle-shaped. On both sides of the proximal end, there is an adjacent medial and lateral facet for the McIII and McV, respectively; they are dorsopalmarly extended and slightly concave; the medial facet is inclined laterally and shorter than the lateral one. The mid-shaft is almost circular in cross-section. The shaft widens in distal direction and is widest at the level of the medial and lateral protuberace for the ligament attachment. The trochlea is higher on the palmar side than on the dorsal side, and the palmar side of the trochlea is divided by a weak sagittal bulge in two halves (medial half is proximally higher than the lateral one) for articulation of the sesamoids.

The McIV of *"M". borsoni* from Kaltensundheim and from Velenje are less stout than that of *M. americanum*, but stouter than that of *Z. turicensis* from Mikulov-Czujan's sandpit. In dorsal view, the proximal end of the McIV of *"M". borsoni* and of *Z. turicensis* only broadens on its lateral side while the medial side is laterally inclined, whereas in *M. americanum* it is extended on both sides. The prox-

imomedial facet for the McIII is more steeply inclined in *"M". borsoni* than in *M. americanum*, which results in a more laterally braced fourth finger in the latter. The lateral facet for the McV is proximodistally higher in *"M". borsoni* than in *M. americanum*, in which it is very low.

Phalanges (Figure 14)

The proximal and medial phalanges of the II, III, and IV left digits (36, 37, 30, 31, 26, 27) are preserved, and all epiphyseal sutures are closed. The proximal phalanges are the widest and deepest proximally, slightly tapering distally; ph1II shows the most pronounced distal tapering among the three proximal phalanges. The ph1III is the biggest and almost symmetrical in dorsal view, ph1 II and IV are smaller and asymmetrical; ph1II is somewhat stretched proximomedially and ph1IV proximolaterally. The proximal facets of all proximal phalanges are oval and dorsopalmarly concave.

The three medial phalanges are smaller than the proximal ones. Among the three medial phalanges, ph2II is the longest (longer than wide) and exhibits the most pronounced distal taper, ph2III the widest (wider than long), and ph2IV the smallest (wider than long). Ph2III is almost symmetrical in dorsal view. In ph2IV the proximal oval facet is slightly laterally inclined. Ph2II is the most asymmetrical and distorted proximolaterally to distomedially, so that the proximal facet is medially inclined.

Hindlimbs

Femur (Figures 5 and 15A-F, Table 3). Both femora are more or less complete; in the left one (4) the area between caput and trochanter major is partialy reconstructed (see Figure 5), in the right one (8) the trochanter major is missing but restored. The trochanter major is distinctly lower than the caput. The caput femoris is hemispherical with only an indistinct notch of the fovea capitis on its mediocaudal margin. The lateral margin of the trochanter major forms a caudally projecting bulge bordering the deeply concave caudal fossa trochanterica. The shaft is slender, straight (in medial/lateral view), and craniocaudally flattened. The tuberositas supracondylaris forms a longitudinal crest along the lateral side of the distal half of the shaft. The distal epiphyseal suture is fused, but still visible. The epicondylus medialis is situated somewhat more proximal than the lateral one and is more swollen. The trochlea femoris is slightly oblique (in cranial view) and inclined proximolateraly; its medial crest is slanting proximolaterally,

whereas its lateral crest is oriented vertically and projecting further distally than the medial one. In caudal view, the medial and lateral condyles are converging in proximal direction. The fossa intercondylaris is therefore very narrow, but deep. The condylus medialis is more massive and distinctly higher in proximal direction than the lateral one. The facies poplitea proximal to the condyles is concave and wide. In distal view, the distal end is almost as wide as deep.

The distal epiphysis (in distal view) of *"M". borsoni* and *Z. turicensis* have almost an equivalent width and depth, whereas in *M. americanum* it is clearly wider than deep. Therefore, also the fossa intercondylis is wider in *M. americanum*, but narrow in *"M". borsoni* and *Z. turicensis*. The size difference between the smaller medial condyle and the larger lateral condyle is more significant in *"M". borsoni* and *M. americanum* than in *Z. turicensis*, in which both condyles have approximatelly the same size. The crest-like tuberositas supracondylaris along the lateral distal half of the shaft is not laterally projecting in *"M". borsoni* and *M. americanum*, but some of the femora of *Z. turicenis* from Mikulov-Czujan's sandpit show a weak or even strong projection in the mid-shaft. A complete femur of *"M". borsoni* is mentioned from Milia (Tsoukala and Mol, 2016), but was not described nor figured and thus cannot be compared.

Tibia (Figure 15G-L, Table 3). The left tibia (5a) is almost complete and preserved in articulation with the fibula, and the right tibia (9) lacks the dorsal part of the proximal epiphysis. The condylus medialis is large, higher than the lateral condyle, and its proximal articular facet is concave and egg-shaped in outline. The condylus lateralis is less high than the medial one, projects laterally, and carries a smaller, oval and concave proximal facet. Both proximal articular facets for the femur raise towards the median and contact each other in a short sagittal crest (eminentia intercondylaris). There is no sagittal furrow (area intercondylaris centralis) between the medial and lateral tuberculum intercondylare, but they are fused to a sagittal crest. Median on the dorsal side of the proximal end the tuberositas tibiae forms a V-shaped bulge split from proximal by a distinct sulcus extensior. A small and slightly concave facet for the articulation with the fibula is situated on the plantar side of the lateral condyle. A longitudinal crest is present along the entire lateral side of the shaft. The plantar surface of the proximal half of the shaft forms a prominent wide furrow, which follows the course of the articulating fibula; the furrow is bordered later-

ally by the above-mentioned lateral crest and medially by a plantar crest, which is very sharp and prominent in the proximal third of the shaft. The gap between tibia and fibula (spatium interosseum cruris) is only open in its distal part, but this is due to the preparation of the fossil bones. The medial side of the shaft is dorsoplantarly deeper than the lateral side, which results in a piriform cross section of the midshaft. The distal epiphysis is somewhat flattened dorsoplantarly. In distal view, the concave cochlea tibiae cover almost the entire distal end, is trapezoid in outline, and slightly tapering medially towards the malleolus medialis. The latter forms a blunt swelling on the medial side, projects distally, and therefore, acts as the medial wall of the cochlea tibiae. A distinct sulcus malleolaris runs on the medial side of the distal end, twists from proximoplantarily to distomedially, and terminates at the malleolus medialis. The distal contact facet for the fibula located in the lateroplantar incisura fibularis, is slightly concave and faces distodorsally; its outline is not well preserved in the right tibia.

The proximal end of the tibia seems mediolaterally more extended in *M. americanum* (caused by a medially more projecting medial condyle) than in *"M". borsoni* from Kaltensundheim and Milia and *Z. turicensis* from Mikulov. In both *"M". borsoni* from Kaltensundheim and *Z. turicensis*, the proximal articular facets contact each other in a sagittal crest (eminantia intercondylaris), whereas they do not contact in *M. americanum,* but are separated by a furrow-like area intercondylaris centralis. The sulcus maleolaris is more prominent in *"M". borsoni* from Kaltensundheim than in *Z. turicensis*.

Fibula (Figure 15H, J, L, Table 3). Only the left fibula (5b), attached to the tibia, is preserved but lacks its proximal end. The slender shaft thickens in distal direction and terminates in a thickened distal end with the malleolus lateralis on its lateral surface. In distal view, the contact line of the medial side of the fibula to the tibia is slightly concave. The distal articular facet for the calcaneus is semicircular in shape and concave. The articular facet for the astragalus is approximately of same size, but flatter. These two facets contact each other along their plantar halves in an almost right angle, but are separated in their dorsal halves by a sulcus. Due to the articulation of the fibula with the tibia the medial side cannot be seen.

The distal articular facets for the astragalus and calcaneus in *"M". borsoni* from Kaltensundheim are almost perpendicular, but are more obtuse in *Z. turicensis* and *M. americanum*.

DISCUSSION

Taxonomic Identification

Zygodont molars identify the skeleton from Kaltensundheim as a typical mammutid proboscidean. The fauna of the Kaltensundheim sinkhole is assigned to the Late Pliocene (MN16-17). During that time, *"M". borsoni* is the only mammutid species known from Europe.

It is generally accepted that *"M". borsoni* in Eurasia and *Mammut americanum* from North America represent two geographically separated terminal species of Mammutidae (e.g., Saunders 1996; Tassy, 1996a; Shoshani and Tassy, 1996; Markov, 2004). Both were attributed to the genus *Mammut* although the genus name is linked to the North American lineage by the type species *M. americanum*. The availability of the genus name *Mammut* for European specimen depends on the phylogenetic hypothesis.

Some authors favor a separate evolution of New and Old World mammutids. During the lower Miocene *Zygolophodon* invaded North America and gave rise to the North American *Mammut* (e.g., Saunders, 1996; Markov, 2004; Koenigswald et al., 2020, acc). The European lineage is assumed to have evolved independently. Therefore, the genus *Mammut* could not originate in two different continents. According to an older hypothesis (e.g., Schlesinger, 1922; Tobien, 1975, 1977) the Eurasian *"Mammut" borsoni* (or *praetypicum/obliquelophus* if valid) entered North America in a second immigration phase during the late Miocene/Pliocene. Such a second immigration, however, lacks any evidence, so far. Other authors were waiting for better finds before the one or another hypothesis can be accepted (e.g., Tassy, 1996a; Shoshani and Tassy, 1996).

We follow the solution of Markov (2004, 2008), using the genus name *"Mammut"* with quotation marks, it shall focus the taxonomic problem and indicate that the mammutid species from Kaltensundheim does not represent the North American genus automatically.

The molars of the Kaltensundheim specimen show the typical characters for mammutids: (Tobien, 1975, 1996; Tassy, 1985): sharp crested lophids, almost completely reduced pretrite conules (crescentoids), open transverse valleys, zygodont crests on posterior slops of postrite main cusps. The m3 differs from those of *Z. turicensis* by its relative larger width and the relatively increased height of the lingual crown-base compared to the height of the lingual (posttrite) lophids (Figure 7).

The molar dimensions are in the range of the *"M". borsoni* group (Figure 16, Table 7). The ranges of molar lengths are almost the same in *Z. turicensis* and *"M". borsoni*, but the m3 of the *"M". borsoni* group are generally wider, although there is overlap. Within the *"M". borsoni* group, the Kaltensundheim m3 is distinctly smaller than the m3 from Milia (Table 7). The relatively short symphysis (Table 8) with two mandibular tusks corresponds with *"M". borsoni* and is shorter than in *Z. turicensis* and also slightly shorter than in the specimens referred to *"M". obliquelophus* and *"M". praetypicum* (Nikolov and Kovačev, 1966; Kubiak, 1972; Mucha, 1980; Markov, 2008). Even if this last character shows significant population-level variability, all morphological characters of the dentition and the mandible as well as the stratigraphic position support the assignment to *"M". borsoni*.

The m3 of the Kaltensundheim mandible lies within the range of the smaller sized specimens of *"M". borsoni* (Figure 16). The molars from the locality Milia in Greece are all larger, especially longer, but they are similar in their length-width ratio (Table 7). The overlap of the dimensions between *Z. turicensis* and *"M". borsoni* is affected by the general variability of the molar dimensions within each taxon and also by their sexual dimorphism, but might also be affected by a slight evolutionary trend characterized by an increasing molar size between the two species according to their stratigraphic position. However, within the tooth-size range of *"M". borsoni,* the m3 from Kaltensundheim is distinctly smaller than those from the stratigraphically older site Milia in Greece (MN15). The metrical variability of the m3 of *"M". borsoni* covers almost the same range as *M. americanum* (Figure 16, metrical data of *M. americanum* taken from Dooley et al., 2019, Figure 32).

Detailed comparisons for each bone with other mammutid taxa are given above. Such comparisons are hampered by the fact that postcranial material and descriptions of mammutid taxa are quite limited. Furthermore, the skeletal remains of compared mammutid taxa represent single individuals or very few individuals, which reduces our knowledge of morphological variability for the different species.

We describe above the few morphological differences of the various bones between the studied specimen of *"M". borsoni* from Kaltensundheim and the other mammutid taxa. In most of the studied bones (ulna, radius, Ci, Cu, CIII, McI, femur) and forelimb skeleton (Figure 9) grater similarity with the *M. americanum* than with ancestral *Z. turicen-*

sis was observed. Such similarity is in agreement with monophyly of the genus *Mammut* proposed by e.g., Schlesinger (1922) or Tobien (1977), but greater similarity with *Z. turicensis* than with *M. americanum*, found in humerus and tibia, imply a parallel evolution of geographically separate evolutionary lineages of Mammutids proposed e.g., by Saunders (1996) or Markov (2004). Parallel evolutionary trends (in this case most probably tied to increasing of body size and lengthening of limbbones with shortening and broadening of the feet) in several groups of proboscideans is well documented (e.g., Shoshani and Tassy, 1996). However, one has to be aware that the range of morphological variability in these features in each taxon is unknown. Therefore, nature of all observed characters must be tested in further studies.

Differences between *Mammut americanum* and the elephantid *Mammuthus primigenius* are much more obvious as illustrated by Olsen (1972). In comparison to the Elephantidae, the skeletal bones of most Mammutidae were sturdier (Warren, 1852; Osborn, 1936; Haynes, 1991). The long bones are more massive, which is expressed in a much higher circumference of the diaphysis (Christiansen, 2007: Figure 3). It is unclear, however, how differences in body mass are reflected in the skeletal elements of the manus. In order to make better comparisons between taxa, a detailed description for the available bones of *"M". borsoni* from Kaltensundheim is provided.

"Mammut" borsoni from Milia was larger than most extant elephants, *Loxodonta africana* and *Elephas maximus* (Larramendi, 2016). However, the fossil elephantid *Palaeoloxodon antiquus* was even larger (Larramendi, 2016). Two different values are suitable to compare the size of proboscideans, the shoulder height and the body mass. The ratio of these values cannot be transferred from extant proboscideans to the fossil ones, because of the varying body proportions (Christiansen, 2004, 2007; Larramendi, 2016; Larramendi et al., 2017) (Figure 17, Table 9 and 10).

The Kaltensundheim Individual

Body size and mass. It is tempting to calculate the body size and body mass from the dimensions of long bones using extant elephants as a model. The ratio between the dimension of the bones and the presumed body size was traditionally extended to fossil proboscideans (Osborn, 1942). Christiansen (2004) derived formulae from *Loxodonta africana* and *Elephas maximus* to calculate the body
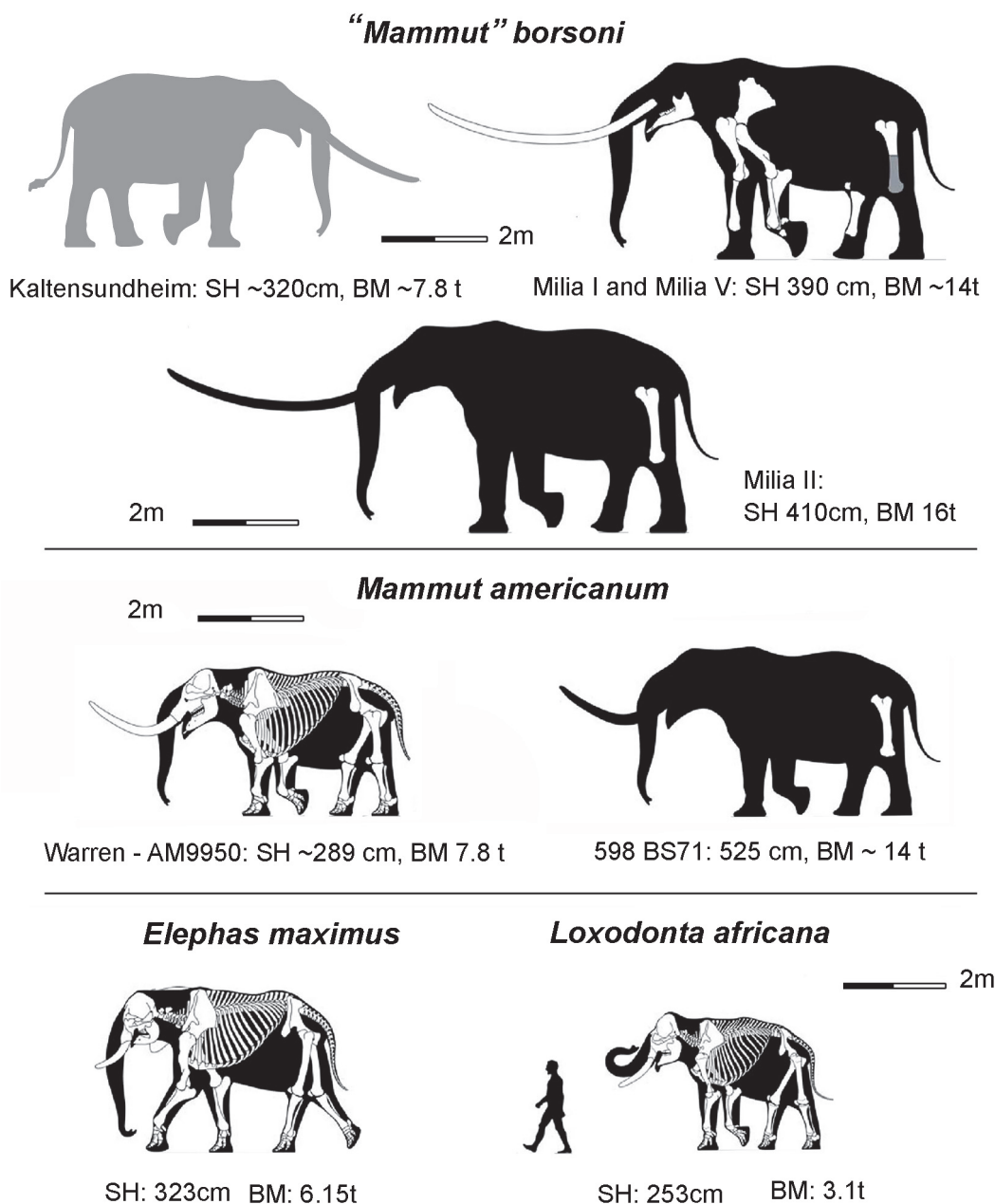
"Mammut" borsoni

Kaltensundheim: SH ~320cm, BM ~7.8 t   Milia I and Milia V: SH 390 cm, BM ~14t

2m

Milia II:
SH 410cm, BM 16t

2m

Mammut americanum

2m

Warren - AM9950: SH ~289 cm, BM 7.8 t   598 BS71: 525 cm, BM ~ 14 t

Elephas maximus   Loxodonta africana

2m

SH: 323cm   BM: 6.15t   SH: 253cm   BM: 3.1t

FIGURE 17. Comparison of the body size in various proboscideans. The silhouettes are from Larramendi, 2016. The one for Kaltensundheim (gray) is adjusted to the predicted shoulder height in flesh 320 cm. *"Mammut" borsoni* was larger than most individuals of *Mammut americanum*. **Abbreviations:** BM – predicted body mass, SH – shoulder height.

mass from various measurements of each long bone (Table 9 and 10). He demonstrated the great significance of the circumference of bones carrying the body. The results may indicate relative size on the order of magnitude. However, Larramendi (2016) demonstrated with more detailed studies that such calculations are not very accurate, for two reasons: most fossil proboscideans differ in their proportions from extant Elephantidae, and most data for Elephantidae were derived from zoo animals, which do not represent natural conditions (Larramendi, 2016). The skeletal shoulder height is calculated as the sum of the length of manus, radius, humerus, and scapula. The living height is estimated to be 5.5 % larger, because of included skin, muscles, and cartilage Larramendi (2015).

TABLE 9. Prediction of the body mass (t) of the individual of *"Mammut" borsoni* from Kaltensundheim according to different methods. **A:** Calculated reconstruction of body mass (t) for the individual of *Z. borsoni* from Kaltensundheim based on different measurements of long bones, using the formula provided by Christiansen (2004): log Body mass = a + b (log x), where x is the relevant measurement. We used those measurements that were claimed by Christiansen (2004: 533) to be the most significant. The formula was deduced by Christiansen (2004) based on extant elephants (*Elephas maximus* and *Loxodonta africana*), and thus the results for *Zygolophodon borsoni* might deviate due to somewhat different body/bone proportions. **B:** Reconstruction of body mass (t) using the equations provided by Larramendi (2016: 552) for adult *Zygolophodon borsoni*. Besides the estimated shoulder height of 300 cm, values for a smaller and a larger shoulder height were calculated.

A Bone, measurement	mm	$\log_{10}$	formula from Christiansen 2004	Body mass Log_{10}	Body mass in tons
Humerus dext, min. circumference	524	2.7193	-1.598 + 2.062 (log x)	4.009	10.2
Humerus dext, min. depth diaphysis	140	2.1461	-0.503 + 2.009 (log x)	3.8	6.4
Radius sin, max. length	790	2.8976	-3.838 + 2.634 (log x)	3.794	6.2
Radius sin min. circumference	210	2.3222	-0.754 + 2.001 (log x)	4.646	6.2
Ulna dext, length	890	2.949	-4.135 + 2.647 (log x)	3.672	4.7
Ulna dext, min. circumference	250	2.3979	-1.349 + 2.022 (log x)	3.499	3.2
Femur sin, physiol. length	1230	3.0899	−5.568 + 3.036 (log x)	3.812	6.5
Femur dext, depth diaph.	100	2	-0.912 + 2.315 (log x)	3.718	5.2
Tibia sin, physiol. length	740	2.8692	−3.064 + 2.378 (log x)	3.759	5.7
Tibia sin, max. length	850	2.9294	−3.064 + 2.378 (log x)	3.902	7.9
Tibia dext, min. circumference	390	2.5910	-2.724 + 2.647 (log x)	4.135	13.6
Mean					**6.8**

B Shoulder height in cm	formula from Larramendi 2016	Body mass in tons
290 cm		6.565
300 cm	$BM = 3.11 \times 10^{-3} \times SH^{2.569}$	7.185
320 cm		8.481

Osborn (1942) estimated this height increase to be 6.33 %. Larramendi (2016) investigated the relationship of length in the different long bones in different proboscideans. He found very strict correlations that help to reconstruct missing elements: e.g., the length of the median metacarpal (McIII) makes up half of the manus height; the height of the manus equals exactly half of the maximal radius length, and thus the radius length is four times the McIII length.

A. Larramendi (Donostia, Spain) kindly proposed different ways to calculate the shoulder height and the body mass of the Kaltensundheim specimen based on our measurments (A. Larramendi, pers. comm. March 4, 2020). The length of the humerus contributes 33.5 % of the skeletal shoulder height, and this value results for the Kaltensundheim specimen 301 cm and correspondingly 318 cm of shoulder height in flesh (Table 9B).

Various other calculations result in a height estimate that is the same order of magnitude. Very precise measurements are avoided here because differences between left and right sides occur, and the McIII is more than the postulated one-fourth of the radius length.

TABLE 10. Selected measurements and calculated shoulder height (cm) of the long bones of *"Mammut" borsoni* from Kaltensundheim, in comparison to different individuals from Milia (GR). (Data from Milia: Tsoukala and Mol, 2016; Larramendi, 2016).

	Kaltensundheim			Milia (GR)			
	max length	physiol. length	min. circumf.	Indiv 1 max length	Indiv. 2a max. length	Indiv 2b max length	Indiv. 5 max. length
Scapula							
Humerus dext	107	97	52,5				
Humerus sin	~101	100		125	108		122.5
Radius dext	~77						
Radius sin	79	73	21				97
Ulna dext	89	74	25				
Ulna sin	92	76					
MC III							
Femur dext	125	119	46,5				
Femur sin	127	123	47			150	
Tibia dext	80		39	87			
Tibia sin	85	74	39				
Skeletal shoulder height	301			390	390		410
Living shoulder height	318						

Following Christiansen (2004), calculating the single bone measurements results in a mean body mass of about 6.8t (ranging between 3.2t-13.6t) for the Kaltensundheim specimen (Table 9). Assuming a shoulder height of about 320 cm allows to calculate a body mass of 7.8t using the formula ($BM=4.16 \times 10^{-3} \times SH^{2.903}$) given by Larramendi (2016, tabl. 7) for fully grown average sized individuals. In addition, Larramendi (pers. comm.) pointed out that the proportions in hind limbs differ somewhat in the Kaltensundheim specimen from those in Milia indicating somewhat higher mass for the Kaltensundheim individual. Accordingly, he modified the kindly provided silhouette (Figure 17). Another method of body mass estimations for proboscideans was provided recently by Jukar et al. (2018) using the breadth of the occipital condyles. However, because the cranium of the Kaltensundheim specimen is not available, we cannot apply this method.

Individual age and cause of death. The Kaltensundheim individual was fully grown. The epiphyseal sutures of all preserved long bones and metapodials are well ossified. The dentition provides further indications: The m1 is shed, the m2 is deeply worn, but still in place, both m3s are fully erupted, but show little wear on the anterior-most lophids.

The individual from Kaltensundheim described here corresponds to class XVIII (out of the serie of I-XXIII) in Tassy's classification (Tassy, 1996b, 2013) established for *Gomphotherium angustidens*. Laws (1966) established an age ranking for *Loxodonta africana* using the eruption and abrasion of the molars. These age groups are widely used for characterizing the individual ages of fossil elephantids. Although Mammutidae chew differently from Elephantidae, Laws's age classes are also applied to *Mammut americanum* (Saunders, 1977; Fisher et al., 2014). The resulting African Elephant Years (AEY) do not refer to astronomical years when applied to other taxa, but they form a valuable basis for comparisons. The Kaltensundheim specimen can be attributed to Laws's age class XIX, which corresponds to 30 AEY. Its wear stage represents an early stage 3 of individual dental age stages (IDAS), established by Anders et al. (2011). The IDAS were defined for dentitions with a normal tooth exchange, but may be used even for taxa with a horizontal tooth replacement.

A survey of mammutid dentitions brought only a few examples of deeply worn last molars, thus most animals died before their dentition was worn out.

Thus, the Kaltensundheim specimen was a fully-grown, midlife individual, but far from senile.

The preservation of entire skeletons in the sinkhole indicates potential reasons for their death. Probably, individuals entered the water hole and were not able to escape from the trap. The situation is similar to the Mammoth Site in Hot Springs (South Dakota, US) (Agenbroad and Mead, 1994), where warm water attracted the animals. In Kaltensundheim, the water in the sinkhole may have been attractive for the animals, because of dissolved salts from the underlying Triassic.

Sex. In proboscideans, adult male and female individuals differ in various characters, such as the pelvis, the skull, the tusk size, and the general body size (e.g., Lister and Agenbroad, 1994; Lister, 1996; Tassy, 1996b, 2013; Göhlich, 2000). In the Kaltensundheim specimen, pelvis and upper tusks are not preserved. *"Mammut" borsoni* is represented in Milia by several individuals of a similar individual age (Tsoukala et al., 2010; Tsoukala and Mol, 2016). The specimen Milia I, II, and V, are regarded as males (Larramendi, 2016: 571). The male character of MIL 5 is accentuated by enormous upper tusks that reach 5 m in length (Tsoukala and Mol, 2016). In comparison to the Milia individuals the Kaltensundheim specimen was smaller. Its humerus is about, 10-20% shorter than those from Milia, and the lower m3 from Kaltensundheim is distinctly smaller than those from Milia (Figure 17, Tables 3 and 10). Therefore, it is tempting to interpret the Kaltensundheim individual as a female. On the other hand, it is assumed that female individuals have smaller or no mandibular tusks (Březina, 2014). We are not certain, whether the linked differentiation forms a bimodal sexual dimorphism (male/female), or if there is only a trend that symphysis and the mandibular tusks are more reduced in females. We observed the phenomenon of a synchronous occurrence of mammutids with and without mandibular tusks is in Europe (e.g., Mikulov-Czujan's sandpit, CZ; Wolkersdorf, AT; d'Autrey, F) and North America (Oregon, USA) (Koenigswald et al., in press). The tuskless mandibles might represent the maximal degree of reduction, which occurs in some female individuals only, whereas others have just smaller mandibular tusks compared to male individuals. In any case, a sexual differentiation has to be considered when discussing Miocene Mammutidae. Therefore, some of the described taxa based on tuskless mandibles, e.g., *Pliomastodon furlongi* Shotwell and Russel, 1963 from Oregon or *Sinomammut tobieni* Mothé, et al., 2016 from China have to be reconsidered.

CONCLUSION

The partial skeleton from Kaltensundheim represents a fully-grown individual of the species *"Mammut" borsoni*. It is smaller than the bulls from Milia and most probably belongs to a female. The animal was trapped in a sinkhole, which yielded a second mammutid, and other floral and faunal remains indicating a pond. The late Pliocene to early Pleistocene age (MN 16-17) is estimated from the floral and faunal biostratigraphical content. The detailed description provides new anatomical details of the postcranial skeleton of *"Mammut" borsoni*, especially in the hand. Postcranial elements of the Kaltensundheim specimen and the compared mammutid species reveal surprisingly more similarities between *"M". borsoni* and *M. americanum* than to *Z. turicensis*. The similar dental and postcranial features in *"M". borsoni* and *M. americanum* have to be regarded as parallel evolution of New and Old World Mammutids. Such parallel evolutionary trends are observed frequently in proboscidean phylogeny (Shoshani and Tassy, 1996). A comprehensive cladistic phylogenetic analysis for mammutids would be highly desireable, however, it is limited by the rarity and incompleteness of the available material.

ACKNOWLEDGEMENTS

Bonn) kindly supported us in handling the 3D models and providing photos. We experienced various technical support from P. Göddertz and G. Olschinski, (Bonn).

Cordial thanks to all of them, especially to the three anonymous reviewers for their valuable comments.

REFERENCES

Ábelová, M. 2003. Mastodonty *Anancus arvernensis* a *Mammut borsoni* (Proboscidea) z lokality Hajnáčka. Morfológia a metrika zubov a postkraniálneho skeletu. Unpublished Master Thesis, Department of Geology and Paleontology, Faculty of Natural Sciences, Comenius University in Bratislava, Slovakia.

Adrover, R. 1962. Hallazgo de restos de mastodonte en las arcillas rojas de Teruel. Revista Teruel, 27:1-6.

Adrover, R. 1963. Estado actual de las investigaciones paleontologicas en la provincia de Teruel. Revista Teruel, 29:1-60.

Agenbroad L.D. and Mead, J.I. 1994. The Hot Springs Mammoth Site: A Decade of Field and Laboratory Research in Paleontology, Geology, and Paleoecology. Mammoth Site of Hot Springs, South Dakota.

Anders U., Koenigswald, W. v., Ruf, I., and Smith, B.H. 2011. Generalized individual dental age stages (IDAS) for fossil and extant placental mammals. Paläontologische Zeitschrift, 85:321-341. https://doi.org/10.1007/s12542-011-0098-9.

Bergounioux, F.M. and Crouzel, M. 1961. *Zygolophodon borsoni* Hays du Musée d'histoire Naturelle de Dijon. Bulletin scientifique de Bourgogne, 19:1-20.

Blumenbach, J.F. 1799. Handbuch der Naturgeschichte. J.Ch. Dietrich, Göttingen.

Böhme, G. 1963. Über den Skelettfund eines Pliocerviden aus dem Pliozän von Kaltensundheim (Rhön). Paläontologische Abhandlungen, 1:353-372.

Böhme, G. 1968. Pliozäne und Pleistozäne Reliefentwicklung und die Plio-Pleistozän Grenze in der östlichen Vorderrhön. Unpublished PhD Thesis, Humboldt-Universität Berlin, Germany.

Böhme, G. 1992. Pliozäne Erdfallbildungen in der östlichen Vorderrhön und ihre Bedeutung für die Morphogenese des Gebietes. Zeitschrift für Geologische Wissenschaften, 20:447-454.

Böhme, G. 2002. Amphibienreste aus dem Oberpliozän von Kaltensundheim (Rhön, Thüringen). Mitteilungen des Museums für Naturkunde Berlin, Geowissenschaftliche Reihe, 5:231-238.

Böhme, G. 2007. Kaltensundheim – ein bedeutsamer Ort für die Landschaftsgeschichte der Rhön. Mitteilungen aus dem Biosphärenreservat Rhön, 12:28-35.

Borissiak, A. 1936. *Mastodon atavus* n. sp., der primitivste Vertreter der Gruppe M. angustidens. Travaux de l'Institut paléozoologique de l'Académie des Sciences de l'URSS, 5: 172-234.

Brandt, J.F. 1860. Vorläufiger Bericht über bedeutende Reste eines unweit von Nikolajew entdeckten Skelettes eines *Mastodon*. Bulletin de l'Académie impériale des Sciences de St.-Pétersbourg, II/13:193-195.

Braniek, G. 1995. Fundstellen oberpliozäner Säugetiere im Vorland der Rhön. Jahresbericht Wetterau. Gesellschaft für Naturkunde, 146/147:195–206.

Březina J. 2014. Osteologické zpracování savců z lokality Czujanova pískovna (Mikulov) se zvláštním zaměřením na studium chobotnatců. MS, Diploma Thesis, Department of Geological Sciences, Faculty of Science MU, Brno, 64 pp. (In Czech).

Březina J. and Ivanov M. 2015. Osteology of *Zygolophodon turicensis* (Mammalia, Proboscidea). In 13th Annual Meeting of the European Association of Vertebrate Palaeontologists. Faculty of Natural Sciences and Technology, OU, Opole, 37.

Březina, J., Alba, D.M., Ivanov, M., Hanáček, M., and Luján, Á.H. 2021. A middle Miocene vertebrate assemblage from the Czech part of the Vienna Basin: Implications for the paleoenvironments of the Central Paratethys. Palaeongeography, Palaeoclimatology, Palaeoecology, 575:110473. https://doi.org/10.1016/j.palaeo.2021.110473

Čerňanský, A. 2006. Revision of a mastodon find from the Neogene at Kuzmice near Topol'čany (Slovakia). Slovak Geological Magazine, 12(1):57-62.

Chalwadźiev, M. 1986. Über einen Fund von *Zygolophodon borsoni* (Hays) bei dem Dorf Bossilkowzi, Bezirk Russe. Jahrbuch der Museen in Nordbulgarien, 12:261-271. (with a German summary)

Christiansen, P. 2004. Body size in proboscideans, with notes on elephant metabolism. Zoological Journal of the Linnean Society, 140(4):523-549. https://doi.org/10.1111/j.1096-3642.2004.00113.x

Christiansen, P. 2007. Long-bone geometry in columnar-limbed animals: allometry of the proboscidean appendicular skeleton. Zoological Journal of the Linnean Society, 149:423-436. https://doi.org/10.1111/j.1096-3642.2007.00249.x

Codrea, V.A. and Diaconu, F. 2007. *Mammut borsoni* (HAYS, 1834) from the Early Pliocene of Husnicioara (Mehedinti district, Romania). Studia UBB Geologia, 52(2):73-77. https://doi.org/10.5038/1937-8602.52.2.9

Dooley, A.C. Jr., Scott, E., Green, J., Springer, K.B., Dooley, B.S., and Smith G.J. 2019. *Mammut pacificus* sp. nov., a newly recognized species of mastodon from the Pleistocene of western North America. PeerJ, 7:e6614. https://doi.org/10.7717/peerj.6614

Dubrovo, I.A. and Jakubowski, G. 1988. The carpus morphology of the forest elephant (*Palaeoloxodon*) and its significance for taxonomy. Prace Muzeum Ziemi, 40:65-83.

Duangkrayom, J., Wang, S.Q., Deng, T., and Jintasakul, P. 2017. The first Neogene record of *Zygolophodon* (Mammalia, Proboscidea) in Thailand: implications for the mammutid evolution and dispersal in Southeast Asia. Journal of Paleontology, 91(1):179-193. https://doi.org/10.1017/jpa.2016.143

Duranthon, F., Heizmann, E.P.J., and Tassy, P. 1995. Safari miocène. Muséum d'Histoire Naturelle de Toulouse, Toulouse.

Fejfar, O. 1961. Die plio-pleistozänen Wirbeltierfaunen von Hajnáčka und Ivanovce (Slowakei), ČSR. I. Die Fundumstände und Stratigraphie. Neues Jahrbuch für Geologie und Paläontologie, Abhandlungen, 11:257-273.

Fejfar, O. 1964. The lower Villafranchian Vertebrates from Hajnáčka near Filákovo in Southern Slovakia. Rozpravy Ústředního ústavu geologického, 30:1-115.

Fisher, D.C. 2008. Taphonomy and paleobiology of the Hyde Park mastodon, p. 197-289. In Allmon, W.D. and Nester P.L (eds.), Mastodon Paleobiology, Taphonomy, and Paleoenvironment in the Late Pleistocene of New York State: Studies on the Hyde Park, Chemung, and North Java Sites. Palaeontographica Americana, 61.

Fisher, D.C., Cherney, M.D., Newton, C., Rountrey, A.N., Calamari, Z.T., Stucky, R.K., Lucking, C., and Petrie, L. 2014. Taxonomic overview and tusk growth analyses of Ziegler Reservoir proboscideans. Quaternary Research, 82:518-532. https://doi.org/10.1016/j.yqres.2014.07.010

Gasparik, M. 2001. Neogene proboscidean remains from Hungary - an overview. Fragmenta Palaeontologica Hungarica, 19: 61-77.

Göhlich, U.B. 1998. Elephantoidea (Proboscidea, Mammalia) aus dem Mittel- und Obermiozän der Oberen Süßwassermolasse Süddeutschlands: Odontologie und Osteologie. Münchner Geowissenschaftliche Abhandlungen, A36:1-245.

Göhlich, U.B. 1999. Order Proboscidea, p. 157-174. In Rössner, G.E. and Heissig, K. (eds.), The Miocene Land Mammals of Europe. Verlag F. Pfeil, Munich.

Göhlich, U.B. 2000. On a pelvis of the straight-tusked elephant *Elephas antiquus* (Proboscidea, Mammalia) from Binsfeld near Speyer (Rhineland-Palatinate, Germany). Paläontologische Zeitschrift, 74:205-214. https://doi.org/10.1007/BF02987962

Göhlich, U.B. 2010. Tertiäre Urelefantenfunde aus Deutschland, p. 363-372. In Meller, H. (ed.), Elefantenreich. Landesamt für Denkmalpflege und Archäologie Sachsen-Anhalt, Halle.

Gümbel, F. and Mai, H.D. 2004. Neue Pflanzenfunde aus dem Tertiar der Rhön, Teil 2: Pliozane Fundstellen. Mitteilungen des Museums für Naturkunde Berlin, Geowissenschaftliche Reihe, 7:175-220.

Harzhauser, M., Daxner-Höck, G., and Piller, W.E. 2004. An integrated stratigraphy of the Pannonian (Late Miocene) in the Vienna Basin. Austrian Journal of Earth Sciences, 95(96):6-19.

Harzhauser, M., Kroh, A., Mandic, O., Piller, W.E., Göhlich, U.B., Reuter, M., and Berning, B. 2007. Biogeographic responses to geodynamics: a key study all around the Oligo–Miocene Tethyan Seaway. Zoologischer Anzeiger - A Journal of Comparative Zoology, 246(4):241-256. https://doi.org/10.1016/j.jcz.2007.05.001

Harzhauser, M., Daxner-Höck, G., Göhlich, U.B., and Nagel, D. 2011. Complex faunal mixing in the early Pannonian palaeo-Danube Delta (Late Miocene, Gaweinstal, Lower Austria). Annalen des Naturhistorischen Museums in Wien, 113:167-208.

Haynes, G. 1991. Mammoths, mastodonts, and elephants: biology, behavior, and the fossil record. Cambridge University Press, New York.

Hays, I. 1834. Descriptions of the specimens of inferior maxillary bones of mastodons in the cabinet of the American Philosophical Society, with remarks on the genus *Tetracaulodon* (Godman). Transactions of the American Philosophical Society, 4, 317-339.

Hilgen, F.J., Lourens, L.J., van Dam, J.A. 2012. The Neogen period. p. 923-978. In Gradstein, F.M., Ogg, J.G., Schmitz, M., and Ogg, G. (eds.), The Geologic Time Scale. Elsevier, Amsterdam. https://doi.org/10.1016/B978-0-444-59425-9.00029-9

Holec, P. 1985. Finds of Mastodon (Proboscidea, Mammalia) Relics in Neogene and Quaternary. Sediments of Slovakia (ČSSR). Západné Karpaty, Séria Paleontológia, 10:13-53.

Holec, P. 1996. A Plio-Pleistocene large mammal fauna from Strekov and Nova Vieska, south Slovakia. Acta Zoologica Cracoviensia, 39(1):219-222.

Hünermann, A. 1983. Berühmte Funde fossiler Proboscidea (Mammalia) vor 150 Jahre. Eclogae Geologicae Helvetiae, 76:911-918. http://doi.org/10.5169/seals-165392

Jukar, A.M., Lyons, S.K., and Uhen, M.D. 2018. A cranial correlate of body mass in proboscideans. Zoological Journal of the Linnean Society, 184(3):919-931. https://doi.org/10.1093/zoolinnean/zlx108

Kahlke, H.-D. 1981. Das Eiszeitalter. Urania, Berlin.

Kahlke, R.-D. 1995. Die Abfolge plio/pleistozäner Säugetierfaunen in Thüringen (Mitteldeutschland). Cranium, 12:5-18.

Kahlke, R.-D. 1998.The Dawn of the Quaternary. Paleoenvironmental, stratigraphy and climate. INQA-SEQS (EuroMam)-Symposium, Tegelen/Kerkrade. Mitteilungsblatt des Thüringischen Geologischen Vereins, 8:32-42.

Karl, H.-V., Reich, M., and Strietzel, T. 2013. Die Mastodontenreste im Subherzyn und ein Neufund von *Mammut borsoni* Kerr, 1792 in einer oberpliozänen Spaltenfüllung Thüringens. Neue Ausgrabungen und Funde in Thüringen, 7:21-31.

Kerr, R. 1792. The Animal Kingdom or Zoological System of the celebrated Sir Charles Linnaeus; Class I Mammalia. John Murray, London.

Koenigswald, W. v. 2016. The diversity of the mastication patters in the Neogene and Quaternary Proboscideans. Palaeontographica, A307:1-41. https://doi.org/10.1127/pala/307/2016/1

Koenigswald, W. v., Widga, C., and Göhlich U.B. (in press). New mammutids (Proboscidea) from the Clarendonian and Hemphillian of Oregon – a survey of Mio-Pliocene mammutids from North America. Bulletin of the Museum of Natural History of Oregon.

Konidaris, G.E. and Koufos, G.D. 2009. Proboscidea. In Koufos, G.D. and Nagel, D. (eds.), The Late Miocene Mammal Faunas of the Mytilinii Basin, Samos Island, Greece: new Collection. Beiträge zur Paläontologie, 31:139-155.

Konidaris, G.E. and Koufos, G.D. 2013. Late Miocene Proboscidea (Mammalia) from Macedonia and Samos Island, Greece: preliminary results. Paläontologische Zeitschrift, 87:121-140. https://doi.org/10.1007/s12542-012-0147-z

Konidaris, G.E. and Tsoukala, E. 2020. Proboscideans from the upper Miocene localities of Thermopigi, Neokaisareia and Platania (NorthernGreece). Annales de Paléontologie 106(2):102380. https://doi.org/10.1016/j.annpal.2019.102380

Krakhmalnaya, T. 2008. Proboscideans and ungulates of Late Miocene fauna of Ukraine. In Krempaská, Z. (ed.), Volume of Abstracts of the 6th meeting of the European Association of Vertebrate Paleontologists Spišská Nová Ves, p. 51.

Kubiak, H. 1972. The skull of *Mammut praetypicum* (Proboscidea, Mammalia) from the collection of the Jagellonian University in Cracow, Poland. Acta Zoologica Cracoviensia, 27:305-324.

Lacombat, F., Abbazi, L., Ferretti, M.P., Martínez-Navarro, B., Mouillé, P-E., Polombo, M-R., Rook, L., Turner, A., and Vialli, A.M.-F. 2008. New data on the Early Villafranchian fauna from Vialette (Haute-Loire, France) based on the collection of the Crozatier Museum (Le Puy-en-Velay, Haute-Loire, France). Quaternary International, 179:64-71. https://doi.org/10.1016/j.quaint.2007.09.005

Larramendi, A. 2015. Skeleton of a Late Pleistocene steppe mammoth (*Mammuthus trogontherii*) from Zhalainuoer, Inner Mongolian Autonomous Region, China. Paläotologische Zeitschrift, 89:229-250. https://doi.org/10.1007/s12542-014-0222-8

Larramendi, A. 2016. Shoulder height, body mass, and shape of proboscideans. Acta Palaeontologica Polonica, 61(3):537-574. https://doi.org/10.4202/app.00136.2014

Larramendi, A., Palombo, M.R., and Marano, R. 2017. Reconstructing the life appearance of a Pleistocene giant: size, shape, genderual dimorphism and ontogeny of *Palaeoloxodon antiquus* (Proboscidea: Elephantidae) from Neumark-Nord, 1 (Germany). Bollettino Della Società Paleontologica Italiana, 56:299-317.

Laub, R.S. 1996. The masticatory apparatus of the American mastodon (*Mammut americanum*), p. 375-405. In Stewart, K.M. and Seymour, K.L. (eds.), Palaeoecology and Palaeoenvironments of Late Cenozoic Mammals: Tributes to the Career of C.S. (Rufus) Churcher. University of Toronto Press, Toronto. https://doi.org/10.3138/9781487574154-020

Laws, R.M. 1966. Age criteria for the African elephant *Loxodonta* a. *africana*. East African Wildlife Journal, 4:1-37. https://doi.org/10.1111/j.1365-2028.1966.tb00878.x

Lehmann, U. 1950. Über Mastodontenreste in der Bayerischen Staatssammlung in München. Palaeontographica, A99:121-228.

Lister, A. 1996. Sexual dimorphism in the mammoth pelvis: an aid to gender determination, p. 254-259. In Shoshani, J. and Tassy, P. (eds.), The Proboscidea. Evolution and palaeoecology of elephants and their relatives. Oxford University Press, New York.

Lister, A. and Agenbroad, L.D. 1994. Gender determination of the Hot Spring mammoths, p. 208-214. In Agenbroad, L.D. and Mead, J.I. (eds.), The Hot Springs Mammoth Site: A Decade of Field and Laboratory Research in Paleontology, Geology, and Paleoecology. Mammoth Site of Hot Springs, South Dakota.

Lofgren, D.L. and Anand, R.S. 2011. Partial skull of *Zygolophodon* (Mammalia, Proboscidea) from the Barstow Formation of California. Journal of Vertebrate Paleontology 31:1392-1396. https://doi.org/10.1080/02724634.2011.605192

Lortet, L.Ch.E. and Chantre, E. 1878. Etudes paléontologiques dans le bassin du Rhône, période Tertiaire. Recherches sur les Mastodontes et les Faunes mammalogiques qui les accompagnent. Première partie. Archives du Muséum d'histoire naturelle de Lyon, tome 2, 1878:285-313.

Mai, D.H. 2007. The floral change in the Tertiary of the Rhön Mountains (Germany). Acta Palaeobotanica, 47:135-143.

Markov, G.N. 2004. The fossil proboscideans of Bulgaria and the importance of some Bulgarian finds – a brief review. Historia naturalis bulgarica, 16:139-150.

Markov, G.N. 2008. The Turolian proboscideans (Mammalia) of Europe: preliminary observations. Historia naturalis bulgarica, 19:153-178.

Masini, F. and Sala, B. 2007. Large- and small-mammal distribution patterns and chronostratigraphic boundaries from the Late Pliocene to the Middle Pleistocene of the Italian peninsula. Quaternary International, 160:43-56. https://doi.org/10.1016/j.quaint.2006.09.008

Mazo, A.V. 1981. Estudio taxonómico de los mastodontes (Proboscidea, Mammalia) de la provincia de Teruel (España). Teruel: Revista del Instituto de Estudios Turolenses, 65:169-194.

Mazo, A.V. and van der Made, J. 2012. Iberian mastodonts: Geographic and stratigraphic distribution. Quarternary International, 255:239-256. https://doi.org/10.1016/j.quaint.2011.07.047

Mein, P. 1990. Updating of MN zones, p. 73-90. In Lindsay, E.H., Fahlbusch, V., and Mein, P. (eds.), European Neogene mammal chronology. Plenum Press, New York.

Mein, P. 1999. European Miocene mammal biochronology, p. 25-38. In Rössner, G. and Heissig, K. (eds.), The Miocene Land Mammals of Europe. Verlag F. Pfeil, Munich.

Mothé, D., Avilla, L.S., Zhao, D., Xie, G., and Sung, B. 2016. A new Mammutidae (Proboscidea, Mammalia) from the Late Miocene of Gansu Province, China. Anais da Academia Brasileira de Ciências, 88(1):65-74. https://doi.org/10.1590/0001-3765201520150261

Mucha, B.B. 1980. A new species of yoke-toothed mastodont from the Pliocene of Southwest USSR, p. 19-26. In Quaternary and Neogene faunas and floras of Moldavskaya SSR, Shtiintsa, Kishinev. (In Russian)

Nikolov, I. and Kovačev, D. 1966. Pliozäne Säugetierfauna aus Assenovgrad. Travaux sur la géologie de Bulgarie Série paléontologie, 8:131142.

Obada, T. 2014. Preliminary data on the *Mammut borsoni* (Hays, 1834) from Otman Hill (Colibaşi, Republic of Moldova). Abstract Book of the VIth International Conference on Mammoths and their Relatives. Scientific Annals of the School of Geology, special volume, 102:143-144.

Olsen, S.J. 1972. Osteology for the Archaeologist No.3. The American Mastodon and the woolly mammoth. Papers of the Peabody Museum of Archeology, 56(3):1-46.

Osborn, H.F. 1936. Proboscidea: A Monograph of the Discovery, Evolution, Migration, and Extinction of the Mastodonts and Elephants of the World: Vol. I: Moeritherioidea, Deinotherioidea, Mastodontoidea. American Museum Press, New York. https://doi.org/10.5962/bhl.title.12097

Osborn, H.F. 1942. Proboscidea. A monograph of the discovery, evolution, migration and extinction of the mastodonts and elephants of the world, Vol. II: Stegodontoidea and Elephantoidea. American Museum Press. New York.

Pavlow, M. 1894. Les Mastodontes de la Russie et leurs rapports avec les Mastodontes des autres pays. Mémoires de l'academie imperial des Sciences de St.-Pétersbourgh, I(3):1-43.

Pfeiffer-Deml, T. 2020. Distinction of *Arvernoceros ardei* and *Cervus perrieri* (Cervidae, Mammalia) from the late Pliocene site of Perrier (France) based on the postcranial skeleton: taxonomic and phylogenetic conclusions. PalZ, 94:377-408. https://doi.org/10.1007/s12542-019-00473-y

Pontier, G. 1926. Contribution à l'étude du *Mastodon turicensis* - Schintz. Annales de la Société Géologique du Nord, 51:149-164.

Prothero, E.D., Davis, E.D., and Hopkins, S.B. 2008. Magnetostratigraphy of the Massacre Lake Beds (late Hemingfordian, early Miocene), northwest Nevada, and the age of the "Proboscidean Datum" in North America. New Mexico Museum of Natural History and Science Bulletin, 44:239-246.

Rakovec, I. 1997. About the osteological differences between the species *Bunolophodon* (*Anancus) arvernensis* (Croizet and Jobert) and *Zygolophodon borsoni*. Geološki zbornik, 12:72-104.

Rasmussen, D.T. and Gutierrez, M. 2009. A mammalian fauna from the late Oligocene of northern Kenya. Palaeontographica Abteilung A, 288,1:7-52, https://doi.org/10.1127/pala/288/2009/1

Rögl, F. 1999. Circum Mediterranean Miocene Paleogeography, p. 39-48. In Rössner, G.E. and Heissig, K. (eds.), The Miocene Land Mammals of Europe. Verlag F. Pfeil, Munich.

Sanders, W.J., Gheerbrant, E., Harris, J.M., Saegusa, H., and Delmer, C. 2010. Proboscidea, p. 161-251. In Werdelin, L. and Sanders, W.J. (eds.), Cenozoic Mammals of Africa. University of California Press, Berkeley, CA. https://doi.org/10.1525/california/9780520257214.003.0015

Saunders, J.J. 1977. Late Pleistocene Vertebrates of the western Ozark-Highland, Missouri. Illinois State Museum Reports of Investigations, No. 33. Springfield, Illinois.

Saunders, J.J. 1996. North American Mammutidae, p. 271–279. In Shoshani, J. and Tassy, P. (eds.), The Proboscidea: evolution and palaeoecology of elephants and their relatives. Oxford University Press, Oxford.

Schaarschmidt, F. 1958. Fund eines *Mastodon* in der Rhön. Neue Museumskunde, 1:290-292.

Schinz, H.R. 1824. Naturgeschichte und Abbildungen der Säugethiere. Brodtmann, Zürich.

Schlesinger, G. 1917. Die Mastodonten des k.k. Naturhistorischen Hofmuseums. Denkschriften des k. k. Naturhistorischen Hofmuseums, Geologisch-Paläontologische Reihe, 1:1-230.

Schlesinger, G. 1922. Die Mastodonten der Budapester Sammlungen. Geologica Hungarica, 2(2):1-284.

Shoshani, J. and Tassy, P. 1996. Summary, conclusions, and glimpse into the future, p. 335-348. In Shoshani, J. and Tassy, P. (eds.), The Proboscidea: Evolution and Palaeoecology of Elephants and Their Relatives. Oxford University Press, New York.

Shotwell, J.A. and Russell, D.E. 1963. Mammalian fauna of the upper Juntura Formation, the Black Butte local fauna. Transactions of the American Philosophical Society, 53:42-69.

Smuts, M.M.S. and Bezuidenhout, A.J. 1993. Osteology of the thoracic limb of the African elephant (*Loxodonta africana*). The Onderstepoort Journal of Veterinary Research, 60:1-14.

Smuts, M.M.S. and Bezuidenhout, A.J. 1994. Osteology of the pelvic limb of the African elephant (*Loxodonta africana*). The Onderstepoort Journal of Veterinary Research, 61:51-66.

Tassy, P. 1977. Découverte de *Zygolophodon turicensis* (Schinz) (Proboscidea, Mammalia) au Lieu-Dit Malartic a Simorre, Gers (Vindobonien Moyen): Implications paléoécologiques et biostratigraphiques. Geobios, 10:655-659. https://doi.org/10.1016/s0016-6995(77)80045-4

Tassy, P. 1985. La place des mastodontes miocènes de l'ancien monde dans la phylogénie des Proboscidea (Mammalia): Hypothèses et conjectures. Unpublished PhD Thesis, Université Pierre et Marie Curie, Paris.

Tassy, P. 1990. The "Proboscidean Datum Event": How many proboscideans and how many events?, p. 237-252. In Lindsay, E.H., Fahlbusch, F., and Mein, P. (eds.), European Neogene Mammal Chronology. Plenum Press, New York. https://doi.org/10.1007/978-1-4899-2513-8_16

Tassy, P. 1996a. Who is who among the Proboscidea?, p. 39-48. In Shoshani, J. and Tassy, P. (eds.), The Proboscidea: Evolution and Palaeoecology of Elephants and Their Relatives. Oxford University Press, Oxford.

Tassy, P. 1996b. Growth and sexual dimorphism among Miocene elephantoids: the example of *Gomphotherium angustidens*, p. 92-100. In Shoshani, J. and Tassy, P. (eds.), The Proboscidea: Evolution and Palaeoecology of Elephants and Their Relatives. Oxford University Press, Oxford.

Tassy, P. 2002. L'émergence du concept d'espèce fossile: le mastodonte américain (Proboscidea, Mammalia) entre clarté et confusion. Geodiversitas, 24(2):263-294.

Tassy, P. 2013. L'anatomie cranio-mandibulaire de *Gomphotherium angustidens* (Cuvier, 1817) (Proboscidea, Mammalia): données issues du gisement d'En Péjouan (Miocène moyen du Gers, France). Geodiversitas, 35:377-445. https://doi.org/10.5252/g2013n2a6

Tassy, P. 2014. L'odontologie de *Gomphotherium angustidens* (Cuvier, 1817) (Proboscidea, Mammalia): données issues du gisement d'En Péjouan (Miocène moyen du Gers, France). Geodiversitas, 36(1):35-115. https://doi.org/10.5252/g2014n1a2

Tassy, P. 2018. Remarks on the cranium of *Eozygodon morotoensis* (Proboscidea, Mammalia) from the early Miocene of Africa, and the question of the monophyly of Elephantimorpha. Revue Paléobiologie, Genève, 37:593-607.

Thenius, E. 1978. Neue Säugetierfunde aus dem Pliozän von Niederösterreich. Mitteilungen der Österreichischen Geologischen Gesellschaft, 68:109-128.

Tobien, H., 1975. The structure of the mastodont molar (Proboscidea, Mammalia). Part 2: the zygodont and zygobunodont patterns. Mainzer Geowissenschaftliche Mitteilungen, 4:195-233.

Tobien, H. 1977. Migrations and non-migrations of proboscideans (Mammalia) via Bering Strait land bridge in the late Cenozic. Journal of the Palaeontological Society of India, 20:237-243.

Tobien, H. 1996. Evolution of zygodons with emphasis on dentition, p. 76-85. In Shoshani, J. and Tassy, P. (eds.), The Proboscidea: Evolution and Palaeoecology of Elephants and Their Relatives. Oxford University Press, Oxford.

Tobien, H., Cheng, G., and Li, Y. 1988. Mastodonts (Proboscidea, Mammalia) from the Late Neogene and Early Pleistocene of the People's Republic of China. Part 2: The Genera *Tetralophodon, Anancus, Stegotetrabelodon, Zygolophodon, Mammut, Stegolophodon*. Some generalities on the Chinese Mastodonts. Mainzer Geowissenschaftliche Mitteilungen, 17:95-220.

Tóth, C. 2010a. Miocénne a spodnopliocénne chobotnatce (Proboscidea, Mammalia) Slovenska. Unpublished Master Thesis, Department of Geology and Paleontology, Faculty of Natural Sciences, Comenius University in Bratislava, 223 pp.

Tóth, C. 2010b. Paleoekológia a diverzita neogénnych chobotnatcov (Proboscidea, Mammalia) na slovenskom území Západných Karpát v závislosti od klimatických zmien a biotických interakcií. Mineralia Slovaca, 42:439-452.

Tsoukala, E., 2000. Remains of a Pliocene *Mammut borsoni* (Hays, 1834), from Milia (Grevena, W. Macedonia, Greece). Annales de Paléontologie, 86:165-191. https://doi.org/10.1016/s0753-3969(00)80007-5

Tsoukala, E., Mol, D., with collaboration: Koukousioura, O., Lazaridis, G., Pappa, Sp., Tsekoura, K., van Logchem, W., Vlachos, E., Makridis, V., Bacharidis, N., and Labretsa, D. 2010. The Milia *Mammut borsoni* (Grevena, Macedonia, Greece): Excavation and display of the longest tusks in the world. Quaternaire 3:90-92.

Tsoukala, E. and Mol, D. 2016. The Proboscidea of the Early Villafranchian site of Milia (Grevena, Macedonia, Greece). Quaternary International, 406:4-24. https://doi.org/10.1016/j.quaint.2014.10.026

van der Made, J. 2010. The evolution of the elephants and their relatives in the context of changing climate and geography, p. 340-362. In Meller, H. (ed.), Elefantenreich. Landesamt für Denkmalpflege und Archäologie Sachsen-Anhalt, Halle.

Virág, A. and Gasparik, M. 2012. Relative chronology of Late Pliocene and Early Pleistocene mammoth-bearing localities in Hungary. Hantkeniana, 7/7:27-36.

Vislobokova, I.A. and Sotnikova, M.V. 2001. Pleistocene faunas with proboscideans of the former Soviet Union. p. 157-160. In Cavaretta, G., Gioia, P., Mussi, M., and Palombo, M.R (eds.), The World of Elephants. Proceedings of the 1st International Congress, Rome. Consiglio Nazionale delle Ricerche, Roma.

Vislobokova, I. 2005. On Pliocene faunas with Proboscideans in the territory of the former Soviet Union. Quaternary International, 126-128:93-105. https://doi.org.10.1016/j.quaint.2004.04.017.

Vlačiky, M., Sliva, L., Tóth, C., Karol, M., and Zervanová I. 2008. Fauna a sedimentólogia lokality Nová Vieska (vilafrank, SR). Acta Musei Moraviae, Scientiae Geologicae, 93:229-244. (in Slovak with English summary)

Wang, S.-Q., Zhang, X.-X., and Li, C.-Y. 2020. Reappraisal of *Serridentinus gobiensis* Osborn and Granger and *Miomastodon tongxinensis* Chen: The Validity of Miomastodon. Vertebrate PalAsiatica, 58:134-158. https://doi.org/10.19615/j.cnki.1000-3118.200310

Warren, J.C. 1852. Description of a skeleton of the *Mastodon giganteus* of North America. John Wilson & Son, Boston. https://doi.org/10.5962/bhl.title.62016

Widga, C., Schubert, B., Wallace, S., Haugrud, S., Compton, B., Samuels, J., and Mead, J. 2017. Early Pliocene Mammutidae of the Gray Fossil Site, northeastern Tennessee, USA. VII International Conference of Mammoths and their relatives. Taichung, Taiwan.

Zapfe, H. 1954. Die Fauna der miozänen Spaltenfüllung von Neudorf an der March (ČSR.) - Proboscidea. Sitzungsberichte der Österreichischen Akademie der Wissenschaften, Mathemathisch-naturwissenschaftliche Klasse, Abt.I, 163:77-78.

Zazula, G.D., MacPhee, R.D.E., Metcalfe, J.Z., Reyes, A.V., Brock, F., Druckenmiller, P.F., Groves, P., Harington, C.R., Hodgins, G.W.L., Kunz, M.L., Longstaff, E.F.J., Mann, D.H., McDonald, H.G., Nalawade-Chavan, S., and Southon, J.R. 2014. American mastodon extirpation in the Arctic and Subarctic predates human colonization and terminal Pleistocene climate change. PNAS, 111:8460-16465. https://doi.org/10.1073/pnas.1416072111

Zhang, X. and Wang, S. (2021). First report of *Eozygodon* (Mammutidae, Proboscidea) in Eurasia. Historical Biology, 33(9): 1661-1670. https://doi.org/10.1080/08912963.2020.1723579